การเตรียมฟิล์มนาโนคอมโพสิตของแป้งมันสำปะหลัง/มอนต์มอริลโลไนต์

นางสาวปิยะพร คามภีรภาพพันธ์

วิทยานิพนธ์นี้เป็นส่วนหนึ่งของการศึกษาตามหลักสูตรปริญญาวิทยาศาสตรมหาบัณฑิต
สาขาวิชาวิทยาศาสตร์พอลิเมอร์ประยุกต์และเทคโนโลยีสิ่งทอ ภาควิชาวัสดุศาสตร์
คณะวิทยาศาสตร์ จุฬาลงกรณ์มหาวิทยาลัย
ปีการศึกษา 2546

ISBN 974-17-4850-5

PREPARATION OF CASSAVA STARCH/MONTMORILLONITE NANOCOMPOSITE FILM

Miss Piyaporn Kampeerapappun

A Thesis Submitted in Partial Fulfillment of the Requirements

for the Degree of Master of Science in Applied Polymer Science and Textile Technology

Department of Materials Science

Faculty of Science

Chulalongkorn University

Academic year 2003

ISBN 974-17-4820-5

Thesis title	Preparation of cassava starch/montmorillonite nanocomposite film
By	Miss Piyaporn Kampeerapappun
Field of study	Applied Polymer Science and Textile Technology
Thesis advisor	Associate Professor Kawee Srikulkit, Ph.D.
Thesis co-advisor	Assistant Professor Duanghathai Pentrakoon, Ph.D.

Accepted by the Faculty of Science, Chulalongkorn University in Partial Fulfillment of the Requirement for the Master's Degree.

.....Dean of Faculty of Science
(Professor Piamsak Menasveta, Ph.D.)

THESIS COMMITTEE

.....Chairman
(Associate Professor Saowaroj Chuayjuljit)

.....Thesis Advisor
(Associate Professor Kawee Srikulkit, Ph.D.)

.....Thesis Co-advisor
(Assistant Professor Duanghathai Pentrakoon, Ph.D.)

.....Member
(Associate Professor Paiparn Santisuk)

.....Member
(Assistant Professor Duangdao Aht-Ong, Ph.D.)

ปิยะพร คามภีรภาพพันธ์: การเตรียมฟิล์มนาโนคอมโพสิตของแป้งมันสำปะหลัง/มอนต์มอริลโลไนต์ (PREPARATION OF CASSAVA STARCH/MONTMORILLONITE NANOCOMPOSITE FILM) อ. ที่ปรึกษา: รศ.ดร. กาวี ศรีกูลกิจ อ. ที่ปรึกษาร่วม: ผศ. ดร. ดวงหทัย เพ็ญตระกูล 101 หน้า. ISBN 974-17-4820-5

การเตรียมฟิล์มนาโนคอมโพสิตของแป้งมันสำปะหลัง/มอนต์มอริลโลไนต์ทำโดยเทคนิคการหล่อจากสารละลาย ในงานวิจัยนี้ เป็นการใช้สารอินเตอร์คาเลต (intercalating agent) (ไดเอทาโนลามีนแคทไอออน) ในการลอกชั้นซิลิเกตของแร่มอนต์มอริลโลไนต์เพื่อให้เกิดการกระจายตัวอย่างสม่ำเสมอของอนุภาคระดับนาโนในเมทริกซ์ของแป้งมันสำปะหลัง วิธีการทดลองคือ นำของผสมระหว่างแป้งมันสำปะหลัง มอนต์มอริลโลไนต์ ไดเอทาโนลามีน (อัตราส่วนระหว่างมอนต์มอริลโลไนต์ต่อไดเอทาโนลามีนเป็น 2:1 ซึ่งคำนวณจากความสามารถในการแลกเปลี่ยนแคทไอออนที่เหมาะสมที่สุด) กลีเซอรอลซึ่งเป็นพลาสติไซเซอร์ และน้ำกลั่น ที่มีค่าความเป็นกรดด่างเป็น 7.0 มาผสมด้วยเครื่องปั่นให้เป็นเนื้อเดียวกัน และให้ความร้อนถึงอุณหภูมิเจลลาติไนซ์ (70-80 องศาเซลเซียส) จากนั้น นำสารละลายแป้งที่เป็นเนื้อเดียวกันมาหล่อในแม่แบบอะคริลิก และทิ้งให้แห้งในบรรยากาศปกติ เมื่อฟิล์มแห้งสนิทจึงลอกฟิล์มออกจากแม่แบบ เพื่อทดสอบสมบัติและวิเคราะห์ผลต่อไป

จากการวิเคราะห์ด้วยเทคนิคเอ็กซเรย์ดิฟแฟรกชัน (XRD) พบการเปลี่ยนแปลงโครงสร้างของมอนต์มอริลโลไนต์จากแผ่นที่ซ้อนกันไปเป็นแผ่นเดี่ยว ฟิล์มนาโนคอมโพสิตของแป้ง/มอนต์มอริลโลไนต์ยังแสดงถึงการหายไปของพีก XRD ที่ตำแหน่ง $2\theta = 5.590^\circ$ อันเป็นการบ่งชี้การเกิดการกระจายตัวในระดับนาโนของมอนต์มอริลโลไนต์ นอกจากนี้ ภาพจากกล้องจุลทรรศน์อิเล็กตรอนแบบส่องผ่าน (TEM) ยังสนับสนุนการเกิดการผสมในระดับนาโนของคอมโพสิตอีกด้วย ถึงแม้จะเตรียมนาโนคอมโพสิตได้ แต่ความทนแรงดึงและยังก์มอดุลัสกลับมีผลตรงกันข้ามกับที่คาดไว้ เนื่องจากผลของการพลาสติไซซ์ของไดเอทาโนลามีน ซึ่งส่งผลให้ความสามารถในการยืดดึง ณ จุดขาดที่เพิ่มขึ้นอย่างเด่นชัด นอกจากนี้ การที่ไดเอทาโนลามีนเป็นสารชอบน้ำมาก จึงทำให้สมบัติทางกายภาพ เช่น อัตราการซึมผ่านของไอน้ำและการดูดซึมความชื้นของฟิล์มเพิ่มขึ้น ซึ่งถือข้อด้อยของการนำไปประยุกต์เป็นฟิล์มบรรจุภัณฑ์

ภาควิชาวัสดุศาสตร์	ลายมือชื่อนิสิต.....
สาขาวิชาวิทยาศาสตร์พอลิเมอร์ประยุกต์และเทคโนโลยีสิ่งทอ	ลายมือชื่ออาจารย์ที่ปรึกษา.....
ปีการศึกษา 2546	ลายมือชื่ออาจารย์ที่ปรึกษาร่วม.....

4572386723: MAJOR APPLIED POLYMER SCIENCE AND TEXTILE TECHNOLOGY
KEYWORD: NANOCOMPOSITE, STARCH, MONTMORILLONITE, BIODEGRADABLE

PIYAPORN KAMPEERAPAPPUN: PREPARATION OF CASSAVA STARCH/MONTMORILLONITE NANOCOMPOSITE FILM THESIS ADVISOR: ASSOC. PROF. KAWEE SRIKULKIT, Ph.D. THESIS COADVISOR: ASST. PROF. DUANGHATHAI PENTRAKOON, Ph.D., 101 pp. ISBN 974-17-4820-5

Cassava starch/montmorillonite nanocomposite films were prepared by solution casting technique. This research was focused on the exploitation of an intercalating agent (cationized diethanolamine) to delaminate the layered silicate of montmorillonite in order to homogeneously disperse the nanoparticles in starch matrix. Mixture of cassava starch, montmorillonite (MMT), diethanolamine (DEA) (calculated from the optimum cation exchange capacity of MMT:DEA of 2:1), glycerol as a plasticizer, and distilled water adjusted to pH 7.0 was well mixed with a homogenizer and heated to gelatinize temperature of 70-80°C. The obtained homogeneous starch solution was cast onto acrylic mold and allowed to dry in open air. The dried film was peeled off and subjected to property investigation and characterizations.

The results showed that change in the montmorillonite structure from layered platelets to individually delaminated sheet was characterized by X-ray diffraction (XRD). The starch/montmorillonite nanocomposite film exhibited the complete disappearance of XRD reflection at $2\theta = 5.590°$, indicating the nanoscale dispersion of montmorillonite. Transmission electron microscopy (TEM) results further supported the blend composite occurring at the nanoscale level. Even though the nanocomposite between starch and montmorillonite was achieved but tensile strength and Young's modulus were found to be opposite to an expectation due to plasticization effect of DEA. This also significantly increased the percent elongation at break. Furthermore, due to the strongly hygroscopic nature of DEA, it led to subsequent disappointment that other physical properties such as water vapor transmission rate (WVTR), and moisture absorption were increased which were not desirable properties for packaging films.

Department of Materials Science	Student's Signature…….
Field of study Applied Polymer Science and Textile Technology	Advisor's Signature……
Academic year 2003	Co-advisor's Signature……..

ACKNOWLEDGEMENTS

The author would like to thank many people for kindly providing the knowledge of this study.

And, the most important thing for this completed thesis is the advice and professional aid of my advisors and co-advisor. I would like to express gratitude and appreciation to Associate Professor Dr. Kawee Srikulkit, and Assistant Professor Dr. Duanghathai Pentrakoon

I wish to express my grateful thank to Associate Professor Saowaroj Chuayjuljit, chairman of thesis committee for her valuable advice, I also would like to express my appreciation to Associate Professor Paiparn Santisuk, Assistant Professor Duangdao Aht-Ong, thesis committee members for their invaluable suggestions and guidances.

I truly thank many helping hands throughout my study including Mr. Wiyong Kangwansupamonkon, Miss Pornpen Siridamrong, Miss Somjit Tangchaiwattana, and other students in the Department of Materials Science, Chulalongkorn University

I wish to thank the Department of Materials Science, Chulalongkorn University for facilities.

Finally, I would like to express my greatest appreciation to my family for their support and encouragement.

CONTENTS

Page

CONTENTS (CONTINUED)

CONTENTS (CONTINUED)

Page

LIST OF TABLES

TABLE **Page**

LIST OF FIGURES

LIST OF FIGURES (CONTINUED)

FIGURE **Page**

LIST OF FIGURES (CONTINUED)

FIGURE **Page**

LIST OF ABBREVIATIONS

MMT	:	Montmorillonite
DEA	:	Diethanolamine
GC	:	Glycerol
TPS	:	Thermoplastic starch
WVTR	:	Water vapor permeability
XRD	:	X-ray diffractometer
TEM	:	Transmission electron microscope
SEM	:	Scanning electron microscope
cps	:	Centipoises
MPa	:	Mega pascal
rpm	:	Revolution per minute
et al.	:	*et alii*

CHAPTER I

INTRODUCTION

Over the past half-century, synthetic plastics have become a major new material for everyday life. Much of the growth has taken place at the expense of more traditional materials, such as steel, aluminium, paper, and glass. Synthetic polymers, such as polystyrene (PS), polypropylene (PP), and polyethylene (PE) are resistant to biodegradation. This situation leads to a growing problem of pollution. Therefore, there has been an increasing interest in a development of biodegradable polymers, e.g. synthesis of biodegradable polymers or incorporation of natural products.

Among natural polymers, starch is considered as one of the most promising candidates for the future primarily because of its attractive combination of availability, price and performance.

Cassava starch is produced in tropical countries such as Thailand. Thailand ranks ninth in the world's producer of cassava roots and is the world's largest exporter of cassava products. Quite often, the production of cassava starch exceeds the export and consumption scale resulting in too much surplus and unused cassava products in the country.

Several studies have been carried out on starch-based films obtained by melt processing or casting from a solution or gel with addition of plasticizers [1]. Even so, starch films have poor mechanical properties when compared to those of synthetic polymers. This is due to their hydrophilic nature and their sensitivity to moisture content which are difficult to control. In order to improve mechanical properties and water resistance, starch can be modified by several methods such as blending with synthetic [2-3] or natural polymers [4], preparing in the composite form [5], and by cross-linking [6].

The preparation of starch composites is aimed to improve the mechanical properties of materials. Commonly, addition of inorganic fillers to a polymer matrix has been investigated extensively. Recently, special attention has been paid to montmorillonite minerals in the field of nanocomposites because of their small particle size with extremely large surface area and intercalation properties [7-8].

Montmorillonite is composed of silicate layers that are 1 nm thick in planar structure and 200-300 nm in the lateral dimension [9]. The typical chemical structures of montmorillonite usually consist of two fused silica tetrahedral sheets sandwiching an edge-shared octahedral sheet of either magnesium or aluminum hydroxide. The Na^{+} and Ca^{+2} residing in the interlayer regions can be replaced by organic cations such as alkylammonium ions by a cationic-exchange reaction to render the hydrophilic layered silicate organophilic. The hydrophobic behavior and an increase in spacing between the layers of silicate are important factors which make organophilic montmorillonite compatible with most hydrophobic polymers. As a result, the ultrafine dispersion of the order of a few nanometers can be obtained. The unique properties of nanocomposite, not shared by conventional materials, include mechanical strength, thermal stability, fire retardant, molecular barrier, and corrosion protection properties.

In this research, cassava starch/montmorillonite nanocomposite films were prepared aiming at producing starch based biodegradable plastic. To obtain the starch/clay nanocomposite, the montmorillonite was treated with an intercalant which, in this study, was an aminoalcohol, diethanolamine neutralized by acetic acid to become the quaternary ammonium salt. The casting process was carried out by the thermal gelatinization of starch/intercalated montmorillonite dispersion under applied shear force. The cast film with the thickness 60-80 micron was then subjected to characterization analysis (X-ray diffraction, scanning electron microscopy, and transmission electron microscopy), physical properties (thickness, transparency, water absorption, and water vapor transmission rate), and mechanical properties (tensile test).

CHAPTER II

THEORY AND LITERATURE REVIEW

2.1 Cassava

Cassava (*Monihot esculenta*) is an important food crop in tropical countries such as Brazil, Nigeria, Indonesia, and Thailand. The roots of cassava are rich in starch and consumed as human food or animal feed. Only a small amount of roots is converted into other industrial products. Thailand is the only country where most of the roots are processed into chips, pellets, and starch [10]. Cassava plant and roots are shown in Figure 2.1.

(a) cassava plant **(b) cassava roots**

Figure 2.1 Photographs of cassava plant and roots.

Starch is a biological material and naturally occurs in a wide variety of plants and agriculture crop. Starch can be used in many ways other than as foodstuff (such as glues, coatings, and sizing), and building materials [11]. Pure starch is white, odorless,

tasteless, and neutral powder existing, in fact, as granules that are insoluble in cold water or organic solvent [12]. The shape and size of the granules depend on their types of plant. Starch granules vary in diameter size from about 2 to 150 μm whereas cassava starch granule size ranges from 5 to 35 μm. It is recently indicated that there may be some correlation between the dispersibility of starch and its average granule dimension where larger granule dimension gelatinize more easily than small ones.

Native starch is insoluble in water below their gelatinization temperature. This is a very important property which enables the starch granules to be easily extracted from the plant source in aqueous systems. In addition, the native starches can be chemically modified in suspension or in water and recovered in purified form by filtration, washing with water, and drying.

Starch granules are insoluble in cold water due to the hydrogen bonds, formed either directly via neighboring alcoholic OH groups of the individual starch molecules or indirectly via water bridges. Even though the hydrogen bonding forces are weak, great number of hydrogen bonds appears in starch granule resulting in starch slightly swelling in cold water (10–15% increase in diameter). This swelling is reversible by shrinking back to their original dimensions at drying state.

Gelatinization is defined as the collapse of molecular ordering within the starch granule resulting in irreversible changes such as granule swelling, crystallinite melting, viscosity development, and starch solubilisation. Starch becomes more gel-like in both its properties and appearance during gelatinization. Gelatinization can be initiated by heating in solution, changing pH or by mechanical means such as extrusion [13]. The gelatinization temperature is recorded as a temperature range in which the starch granules loss their birefringence as observed under the microscope. The gelatinization

temperature is a characteristic property of starch. With cassava starch, gelatinization starts and completes at 60°C and 80°C, respectively. The point of gelatinization depends to a certain extent on granule size – the smaller granules being more resistant to swelling [14].

Most starch consists of two structurally different polysaccharides, the linear amylose (normally 20–30%), and the branch amylopectin (normally 70–80%), so the overall behavior of starch is determined by the relative amounts of amylose and amylopectin. Each factor has unique properties that contribute to the functionality of starch from various plant sources.

(a) Amylose

Amylose is a linear component, produced by 1,4-α-D-glucosidic linkage. It is a minor component, amylose content typically ranging from 20% to 30%. Its molecular weight is about 0.2–2 millions. Starch from various sources differs in relative content of amylose. In general, the root and tuber starch contain somewhat less amylose than the cereal starch. Cassava starch has amylose content about 16.5–22%. Chemical structure of amylose is shown in Figure 2.2.

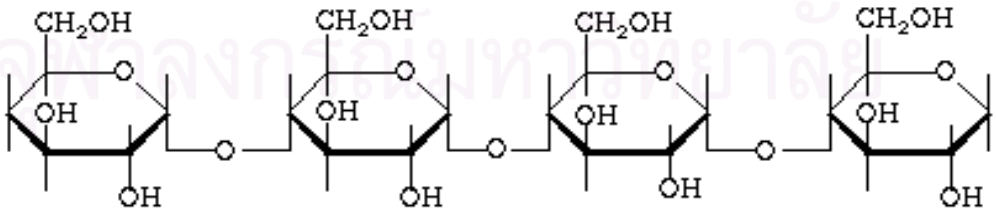

Figure 2.2 Chemical structure of amylose.

(b) Amylopectin

Amylopectin is a branched component which consists of short 1,4-α-linked chains connected to each other by an α(1,6)glucosidic linkage. The molecular weight of amylopectin is about 100–400 millions, but the average chain length is only 20–30 glucose unit. Chemical structure of amylopectin is shown in Figure 2.3.

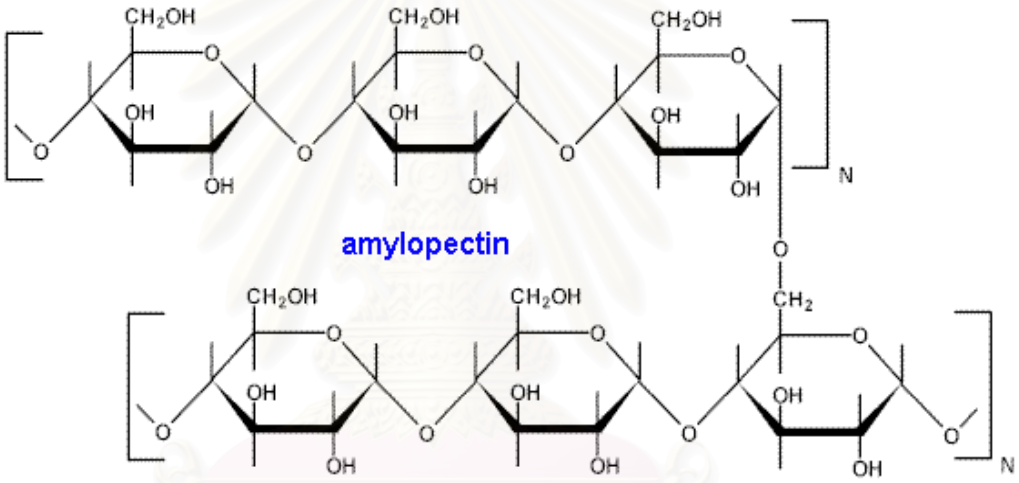

Figure 2.3 Chemical structure of amylopectin.

2.2 Biobased materials

Biobased materials, derived from renewable sources, are normally used for food applications. They may be divided into three main categories based on their origin and production:

♦ Polymer directly extracted/removed from biomass. Examples are polysaccharides (such as cellulose, starch, and chitin) and proteins (such as casein, whey, collagen, and soy). These polymers normally have some difficultly in

processing and final performance as a result of hydrophilic behavior; therefore they generally absorb the surrounding moisture. On the other hand, these polymers have excellent gas barriers.

- Polymers produced by classical chemical synthesis using renewable biobased monomers. A good example is polylactic acid, a biopolyester polymerized from lactic acid monomers. The monomers themselves may be produced via fermentation of carbohydrate fed stock.

- Polymers produced by microorganisms or genetically modified bacteria. To date, this group of biobased polymers consists mainly of the polyhydroxyalkonoates, but developments with bacterial cellulose are progress.

2.2.1 Starch based biodegradable materials

Because the oil embargo in the early 1970s caused the price of plastics to almost double, researchers began to look for less expensive, non-plastic filler. The result of their search was starch-based polymers. Since that time, starch based polymers have remained the most commonly used and lowest-costing ingredient of all biodegradable polymers.

Biodegradable materials are used in the same way as regular materials but can be returned to the environment by being broken down into water and carbon dioxide by microorganisms and naturally occurring degrading enzymes. The natural polymer starch significantly determines the degradability of these plastics. This starch can be derived from many agricultural commodities, including cassava, corn, and potatoes. Although all of these starches are easily digested by microorganisms, each individual type of starch will result in different plastic thicknesses in the final product.

The worldwide consumption of biodegradable polymers has increased from 14 million kg in 1996 to an estimated 68 million kg in 2001. Target markets for biodegradable polymers include packaging materials (e.g. trash bags, wrapping, loose-fill foam, food containers, film wrapping, laminated paper), disposable nonwovens (e.g. engineered fabrics), hygiene products (e.g. diaper back sheets, cotton swabs), consumer goods (e.g. fast-food tableware, containers, egg cartons, razor handles, toys), and agricultural tools (e.g. mulch films, planters) [15].

There are three methods to manufacture starch-based materials:

- Surface-modified starch additive − Starch is treated with small amount of unsaturated fat or a fatty acid oxidizing agent, such as vegetable oil. This agent is added to the mixture to improve its compatibility with the polymer. The obtained material can be molded by conventional methods, such as film blowing, injection molding, and blow molding. The time and extent of degradation depends greatly on the type of polymer, thickness of the material, and environmental conditions.

- Gelatinized starch additive − To increase the amount of starch-based products, the US Department of Agriculture has developed a process using gelatinized starch, both in films of polyethylene-*co*-acrylic acid (EAA) and in a mixture of EAA and low density polyethylene. The material is prepared by premixing 40 to 60% starch with EAA and water. Adding EAA is necessary to make this large amount of starch compatible with the polyethylene. The obtained materials may be used for mulching applications because of transparent and flexible properties.

- Thermoplastic starch materials − Recently, materials have been developed to contain 70–100% starch as the base for the polymer. Not only do these materials use a large amount of starch, but their water-solubility is greatly increased. In

addition, these materials are very easily consumed by microorganisms. Possible markets include mulch films, bags for animal feed and fertilizer, and products that will end up in waterways or wastewater treatment facilities.

2.3 Composites

Humans have been using composite materials for thousands of years. Most composites are made up of just two materials. One material (the matrix or binder) surrounds and binds together a cluster of fibers or fragments of a much stronger material (the reinforcement).

A composite is a heterogeneous substance consisting of two or more materials which does not loss the characteristics of each component. The combination of materials brings about new desirable properties. Within the composite, it is still possible to distinguish the different materials apart. They do not dissolve or blend into each other. The properties of a composite material depend not only upon the properties of the individual component phases (matrix, filler, interphase), but also upon their interaction.

The composite's phase morphology has significant effects on properties and this morphology significantly depends on interphase interaction, if this area of the interface between the two components becomes significantly large [16].

2.3.1 Types of composite

The four major types of matrices are polymer, metallic, ceramic, and carbon.

- **Polymer Matrix Composites (PMC's)**

Polymer resins are broadly divided into two categories: thermosetting and thermoplastic. In thermosetting polymers, resin starts as a liquid and changes to a hard, rigid solid when crosslinks, are formed at the molecular level. The mechanical properties of the matrix depend on the degree of crosslinking. The curing process is critical because it significantly determines the amount of crosslinking. Thermoset materials tend to be brittle. The primary thermoset resins include epoxies (used in aerospace and aircraft), polyester and vinyl esters (used in automotive, marine, chemical and electrical applications), phenolics (used in bulk molding compounds), polyimides, and polybenzimidazoles (for high temperature aerospace applications).

Thermoplastic resins do not form crosslinks. They derive their strength from their particular properties which are determined by their monomer units and their high molecular weight. In general, thermoplastics are impermeable to chemicals and moisture. Because of an absence of crosslinking, thermoplastics will undergo large deformation before fracturing. Thermoplastic resins include nylon, polyethylene terepththalate (PET), polycarbonate (used in injection molded articles), polyamide-imide, and polyether ether ketone (PEEK). Thermoplastic processing is more difficult in general than thermoset one because thermoplastic resins tend to be more viscous. This viscosity makes the resins difficult to impregnate into the reinforcing fibers.

- **Metal Matrix Composites (MMC's)**

Although heavier than PMC's, metal matrix composites possess greater tensile strength, higher melting points, smaller coefficients of expansion, higher ductility and increased toughness. At the present time, the focus seems to be on the development of matrices of aluminum, magnesium and titanium. Methods of

producing these composites include (i) squeeze infiltration – liquid metal is injected into a mat of short fibers, (ii) stir casting – liquid metal is stirred with ceramic particles and allowed to cool, (iii) spray deposition – droplets of metal are sprayed onto a substrate, (iv) powder blending and consolidation – metallic powder is mixed with ceramic fibers or particles, and (v) diffusion bonding of foils – titanium foil is placed along a fiber array and the fibers are then wound and hot pressed.

- **Ceramic Matrix Composites (CMC's)**

Naturally resistant to high temperatures, ceramic materials have a tendency to be brittle and fracture. Composites successfully made with ceramic matrices are reinforced with silicon carbide fibers. These composites offer the same high temperature tolerance of superalloys but without such a high density. The brittle nature of ceramics makes composite fabrication difficult. Usually most CMC production procedures involve starting materials in powder form.

- **Carbon Carbon Composites**

Carbon carbon composites are various forms of carbon fiber. The materials are highly resistant to heat, wear, and fracture. Unlike superalloys and ceramics, they are lightweight and retain their strength at high temperatures, have low coefficient of thermal expansion (CTE), high thermal conductivity (TC), and resist thermal shock. Application areas include friction materials such as high performance clutches, and aircraft brakes.

2.4 Clay minerals

Clay is a cheap natural raw material that has been widely used for many years as filler for rubber and plastic to reduce polymer consumption and cost. Geologists have used the word “clay” in two senses: as a size term, to refer to material of any composition whose average grain size is less than approximately 0.004 mm, and as a mineralogical term, referring to a group of minerals with a specific range of composition and a particular kind of crystallographic structure. The two meanings often overlap or coincide because the fine grained part of a soil or sediment commonly consists largely of clay minerals.

In general, the term clay implies a natural, earthy, fine grained material which develops plasticity when mixed with a limited amount of water. By plasticity, it means that the property of the moistened material is deformed under the application of pressure, with the deformed shape being retained when the deforming pressure is removed. According to chemical analysis of clays, it composes of silica, alumina, and water, frequently with appreciable quantities of iron, alkali, and alkaline earth metals. The two major types of clay minerals are 1:1, and 2:1 type minerals [17].

(a) <u>1:1 type minerals</u>

The 1:1 clay-mineral type consists of one tetrahedral sheet and one octahedral sheet. These two sheets are approximately 7 Å thick as shown in Figure 2.4.

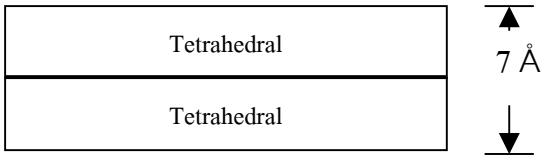

Figure 2.4 1:1 type minerals.

A kaolinite mineral is one of 1:1 type minerals. The structure is composed of a single silica tetrahedral sheet and a single alumina octahedral sheet combined in a unit so that the tips of the silica tetrahedrons and one of the layers of the octahedral sheet form a common layer.

(b) 2:1 type minerals

The three sheets or 2:1 layer lattice silicates consist of two silica tetrahedral sheets between which is an octahedral sheet. These three sheets form a layer approximately 10 Å thick as shown in Figure 2.5.

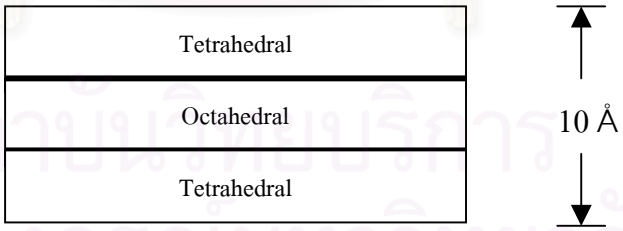

Figure 2.5 2:1 type minerals.

❖ Smectite

Smectite is composed of units made up of two silica tetrahedral sheets a central alumina octahedral sheet. All the tips of the tetrahedral point in the same

direction toward the center of the unit. The tetrahedral and octahedral sheets are combined so that the tips of the tetrahedral. An important clay in this group is montmorillonite as explained in section 2.4.1.

There are many species of clays in a group of smectite clay minerals that consist of many layers of octahedral aluminate sheets sandwiched between tetrahedral silicate layers as presented in Table 2.1 and Table 2.2 shows summary of properties of clay minerals.

Table 2.1 The species in smectite clay group [18]

Subgroup	Species	Ideal Formula
Saponites	Saponite	$Na_{0.6}[Mg_6(Al_{0.6}Si_{7.4})O_{20}(OH)_4]$
	Hectorite	$Li_{0.6}[(Li_{1.6}Mg_{4.4})Si_8O_{20}(OH)_4]$
	Fluorohectorite	$Li_{0.6}[(Li_{1.6}Mg_{4.4})Si_8O_{20}F_4]$
Montmorillonites	Montmorillonite	$Na_{0.6}[(Mg_{0.6}Al_{3.4})Si_8O_{20}(OH)_4]$
	Beidellite	$Na_{0.9}[Al_4(Al_{0.9}Si_{7.4})O_{20}(OH)_4]$

Table 2.2 Summary of properties [19]

Type	Size (μm)	Surface area (m^2/g)		Interlayer spacing (nm)	Cation sorption
		External	Internal		
Kaolinite	0.1 – 5.0	10 – 50	–	0.7	5 – 15
Smectite	< 1.0	70 – 150	500 – 700	1.0 – 2.0	85 – 110
Vermiculite	0.1 – 5.0	50 – 100	450 – 600	1.0 – 1.4	100 – 120
Illite	0.1 – 2.0	50 – 100	5 – 100	1.0	15 – 40

❖ Vermiculite

The structure is unbalanced chiefly by substitutions of Al^{3+} for Si^{4+}. These substitutions may be partially balanced by other substitutions within the mica lattice, but there is always a residual net-charge deficiency of 1 to 1.4 per unit cell.

Vermiculite differs from smectite in that the expansion with water is limited to about 4.98 Å. Vermiculites absorb certain organic molecules between the mica layers but differ from smectite in that the adsorbed layer is thinner and less variable. All these differences may be due to the fact that the unbalancing in the vermiculite perhaps essentially in the tetrahedral layer, whereas in smectite it is mainly in the octahedral layer.

❖ Illite

The basic structure unit is a layer composed of two silica tetrahedral sheets with a central octahedral sheet. The tips of the tetrahedral in each silica sheet point towards the center of the unit and are combined with the octahedral sheet in a single layer with suitable replacement of hydroxyl group by oxygen.

The unit is the same as that for montmorillonite except that some of the silicons are always replaced by aluminums and the resultant charge deficiency is balanced by potassium ions.

2.4.1 Montmorillonite

Montmorillonite has the widest acceptability for use in polymers. It is a type of smectite clay that can absorb water, and it is a layered structure with aluminum octahedron sandwiched between two layers of silicon tetrahedron. Each layered sheet

is slightly less than 1 nm thin (10 Å), with surface dimensions extending to about 1 μm or 1000 nm. The aspect ratio is about 1000 to 1 and the surface area is in the range of 750 m^2/g. SEM micrograph of montmorillonite showing very fine particle size is shown in Figure 2.6.

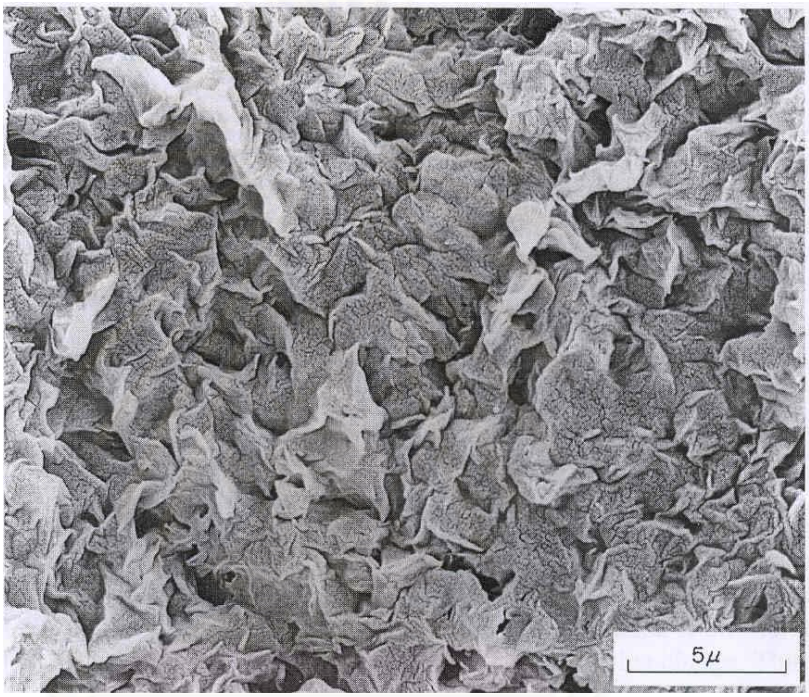

Figure 2.6 SEM micrograph of montmorillonite [8].

Montmorillonite clays are relatively common throughout the world. Deposits of commercial clays are referred to as bentonite, which generally contains in excess of 50% montmorillonite. Conventional purification methods are adequate for the clays used in most common applications, such as binders for metal casting, well-drilling legs, and cosmetics.

Montmorillonite clay is hydrophilic; hence it is not inherently compatible with most polymers and must be chemically modified to make its surface more

hydrophobic. The most widely used surface treatments are ammonium cations which can be exchanged for existing cations already on the surface of the clay. The treatments work on the clay to minimize the attractive forces between the agglomerated platelets.

Montmorillonite is one in smectite group which has a low thermal expansion coefficient and a high gas barrier property. Stacking of this structure leads to a regular weak dipolar or van der waals interaction between the layer. Isomorphic substitution in each layer generates negative charges that are counterbalanced by hydrated sodium or potassium ions residing in the interlayer spaces. Due to this special characteristic, montmorillonite can be easily dispersed in water resulting in a stable colloid. Typically, the natural montmorillonite is too hydrophilic to disperse in an organic matrix. Its dispersibility can be improved to make it useful by ion exchanges with an organic cation molecule, such as cationic surfactant, onto the filler's surface. The arrangement of smectite-clay structure by cation exchanges with cation surfactant is shown in Figure 2.7 [18].

The functions of organic cation molecules in organophilic-clay are to lower the surface free energy of the silicate layers and to improve the wettability behavior of hydrophobic polymer matrix. In addition, the organic cation may contain various functional groups that can react with the polymer molecule to improve the adhesion strength between the inorganic phase and the matrix as reported by Giannelis [18].

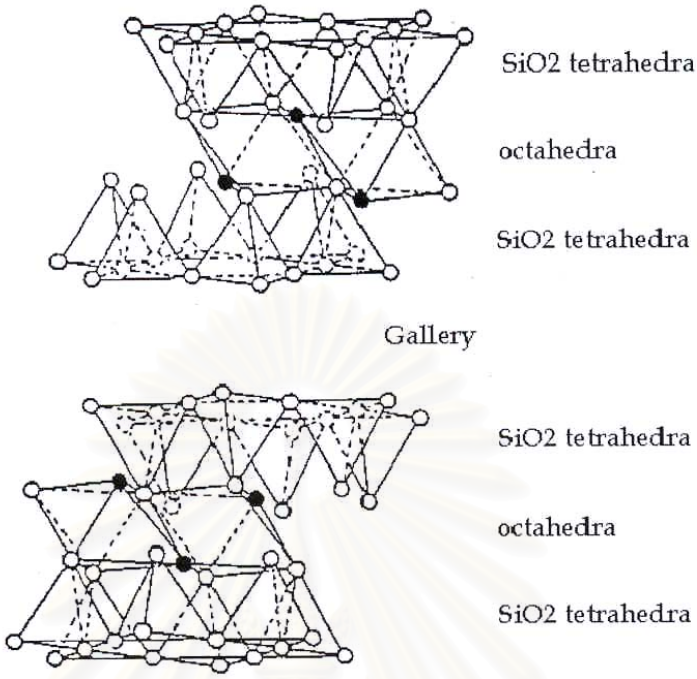

Figure 2.7 Smectite-clay structure [20].

2.5 Nanocomposites

Composites that exhibit a change in composition and structure over a nanometer length, nanocomposites, have been shown over the last 10 years to afford remarkable property enhancements relative to conventionally-scaled composites. Layered silicates dispersed as a reinforcing phase in an engineering polymer matrix are one of the most important forms of such "hybrid organic-inorganic nanocomposites". The term "nanocomposite" describes a two-phase material where one of the phases has at least one dimension in the nanometer (10^{-9} m) range [21].

Generally, polymer layered silicated composites are ideally divided into three types.

❖ Conventional composite composes of silicate tactoids with the silicate layers aggregated in the unintercalated form. Consequently, discrete phases usually take place because of no penetration of polymer molecules into layer silicate phase [22].

❖ Intercalated nanocomposite consists of a regular insertion of polymer in between the silicate layers [21]. The intercalated type of polymer-clay hybrid has been touted to have highly extended single chains confined between the clay sheets, within the gallery regions. The clay sheets retain a well ordered, periodic, stacked structure. The intercalation process can be monitored by tracking the increasing long spacing from X-ray scattering, since the galleries must expand to accommodate larger molecules. In general, the literature defines a polymer-intercalated montmorillonite as having a long spacing less than 20–30 Å [23].

❖ Exfoliated nanocomposite where 1 nm thick layers are dispersed forming a monolithic structure at the microscale. The delaminated or exfoliated structure ideally has well dispersed and randomized (in orientation) clay sheets within a matrix of the "coil-like" polymer chains. In this case the sheets have lost their stacked orientation, and if the structure is truly random then no distinct long spacing should be observable by X-ray scattering. In general, the literature defines a polymer delaminated hybrids having spacing greater than 80–100 Å [23].

The schematic illustrations of the three possible types of polymer-clay hybrids are shown in Figure 2.8 and examples of TEM images of nanocomposite in some researchers are shown in Figures 2.9–2.10.

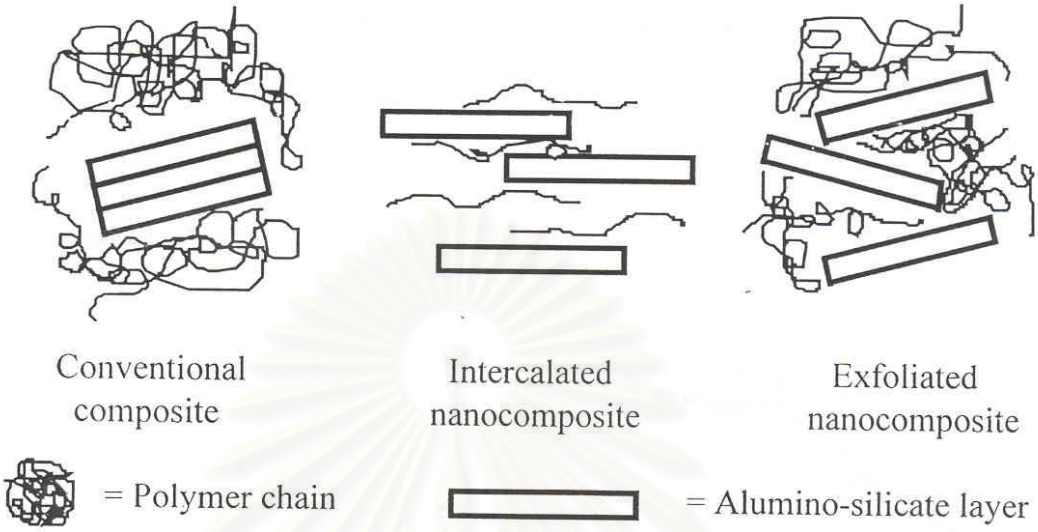

Figure 2.8 Three possible types of polymer-clay composites [18].

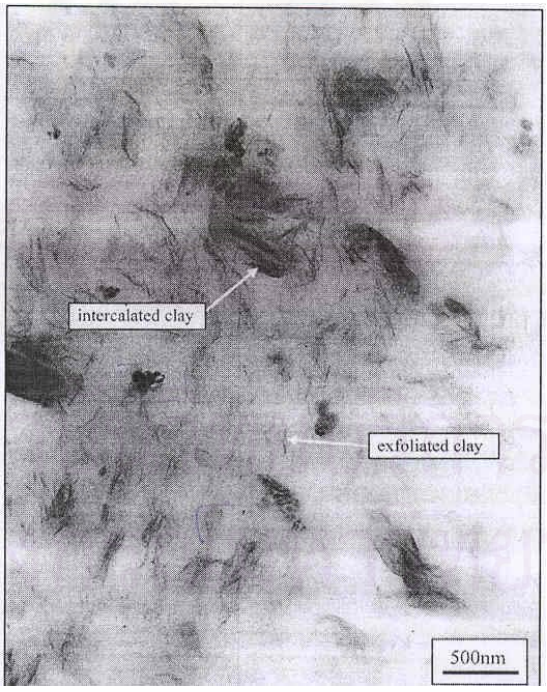

Figure 2.9 TEM image of biodegradable clay nanocomposite prepared by Okada *et al.* as shown intercalated clay and exfoliated clay [24].

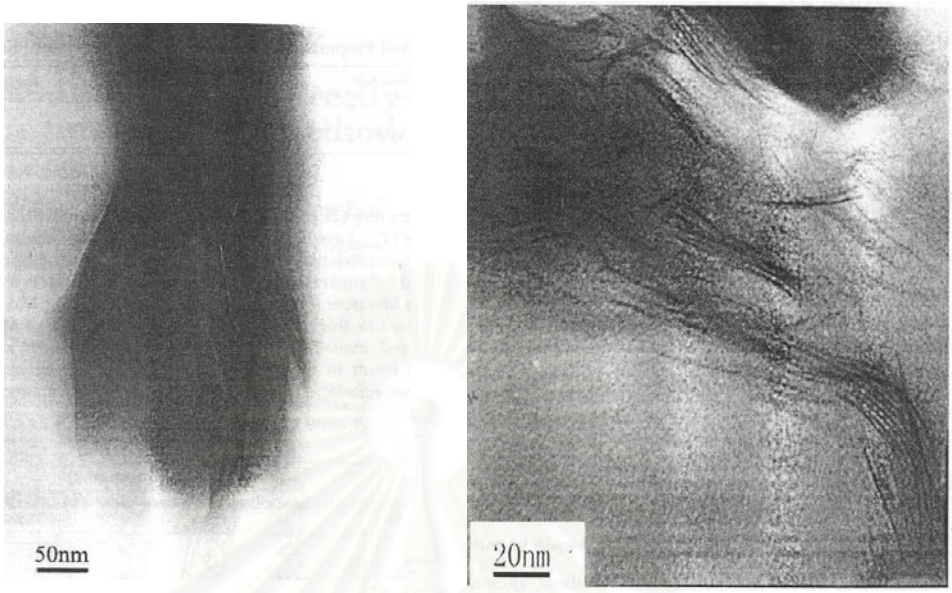

(a) unintercalated (b) intercalated

Figure 2.10 TEM images of PE/clay nanocompsite: (a) unintercalated (b) intercalated prepared by Wang *et al.* [25].

Although the high aspect ratio of silicate nanolayers is ideal for reinforcement, the nanolayers are not easily dispersed in most polymers due to their preferred face-to-face stacking in agglomerated tactoids. Dispersion of the tactoids into discrete monolayers is further hindered by the intrinsic incompatibility of hydrophilic layered silicates and hydrophobic engineering plastics. However, as first being demonstrated by Toyota group more than 10 years ago, the replacement of the inorganic exchange cations in the galleries of the native clay by alkylammonium surfactants can compatibilize the surface chemistry of the clay and the hydrophobic polymer matrix [18].

2.5.1 Synthesis of polymer-layered silicate nanocomposites [21]

There are four different methods to synthesize polymer-layered silicate nanocomposites:

- The solution method, the organoclay, as well as the polymer are dissolved in an organic polar solvent. The entropy gained by the desorption of solvent molecules allows polymer chains to diffuse between the clay layers, compensating for decreased conformational entropy. After evaporation of the solvent, the result is shown an intercalated nanocomposite.
- The *in-situ* polymerization approach is similar to the solution method except that the role of the solvent is replaced by a polar monomer solution. Once the organoclay is swollen in the monomer, the curing agent is added in favorable cases exfoliation occurs.
- The melt intercalation process was first reported by Vaia *et al.* in 1993. The strategy is to blend a molten thermoplastic with an organosilicate in order to optimize the polymer/layered silicate interactions. The process is sufficiently rapid to take place in a conventional mixing extruder.
- The *in-situ* formation of silicate layers is a relatively new approach proposed by Carrado *et al*. They utilize *in-situ* hydrothermal crystallization of silicate layers in an aqueous polymer gel.

2.5.2 Benefits of nanocomposites

Today's nanocomposites typically demonstrate unique improvements in material properties, including rigidity, strength, and barrier characteristics, while maintaining a level of transparency and offering the potential for recyclability.

❖ **Increased rigidity**

Nanocomposite polymers offer increased rigidity and stiffness while maintaining a high degree of the elongation inherent in the base polymer. Increased stiffness without brittleness is essential for many catheter applications, which require torque and push/pull strength without kinking. In addition, new dilation balloons are required to withstand higher pressures without tearing, and may also be excellent candidates for improvement in mechanical performance from nanocomposite technology.

❖ **Permeation resistance**

The platelet structure of the reinforcing fillers in nanocomposites may offer improvement in barrier properties of the polymer compound. To date, much commercial interest in nanocomposites barriers has come from packaging companies.

❖ **Transparency**

With nanocomposites, low loadings and filler dispersion create compounded materials that maintain inherent polymer transparency in thin sections. This is an additional benefit for packaging and film applications.

❖ **Recyclability**

A major difference in compounding nanoclays versus other types of reinforcement fillers is that with nanoclays, typical fibers are broken down during the high-shear compounding operation but nanoparticles are not affected or degraded during the process. This allows nanocomposites to be recycled and reprocessed without seriously affecting the physical properties. Performance enhancements with nanoclays vary among polymers. For instance, nylons will accept nanoclays more readily than polypropylene, in which dispersion is currently difficult to achieve.

2.6 Literature Reviews

Abdul [26] prepared organic compound of bentonite (clay). The expansion of silicate layer depended on the length of hydrocarbon. The expansion of layer was multiple of 4 Å, which was about the thickness of one hydrocarbon chain. Moreover, the swelling ability of organic bentonite in various organic solvents was studied. Binary solvents showed better achievement to swell the organic compound of bentonite than monosolvent systems.

Jin-Ho Choy *et al*. [27] reported the dispersion of quaternary alkylammonium modified montmorillonite in polar and nonpolar solvents. It was showed that the dispersibility of modified montmorillonite depended on compatibility between functional group on the modifying agent and type of solvents.

Yang *et al*. [28] discussed about influence of intercalation agent on the structure of montmorillonite (MMT). The wide angle X-ray diffraction (WAXD) patterns showed the basal spacing of MMT with various intercalation agents. The basal spacing of MMT was increased by the organo-modification. For certain type of intercalation agent, the basal spacing of organo- modified MMT increased with length of the alkyl group in an agent.

Polyimide hybrid with montmorillonite clay mineral was synthesized from dimethylacetamide (DMAC) solution of poly (amic acid), and a DMAC dispersion of montmorillonite intercalated with an ammonium salt of dodecylamine by Yano *et al.* [29]. Montmorillonite consisted of stacked silicate sheets about 2000 Å in length, 10 Å in thickness. The organophilic-clay was uniformly dispersed in a polyimide film. This

hybrid or nanocomposite material showed excellent gas barrier properties, and low thermal expansion coeffient compared to an ordinary polyimide.

Poly(ε-caprolactone)-clay nanocomposites using 12-aminododecanoic acid together with concentrated hydrochloric acid as a cation exchanging reagent in sodium montmorillonite (clay) was prepared by Messersmith and Giannelis [30]. The results from wide angle X-ray scattering (WAXS) showed that the alumino-silicate layers produced fine dispersion in polymer matrix. The significant property of nanocomposites was a reduction in moisture permeability.

Pinnavaia *et al.* [31] prepared epoxy-clay nanocomposites by *in-situ* polymerization of epoxy resin monomer in different types of organophilic-clay. Both the tensile strength and the modulus increased with increasing clay content. The reinforcement provided by the silicate layers at 15 wt% loading was manifested by a more than tenfold improvement in tensile strength.

Giannelis [32] prepared poly (ethylene oxide)-clay nanocomposite by direct polymer melt intercalation. This process involved mixing the layer silicate with the polymer and heating the mixture above the softening point of the polymer. Differential scanning calorimetry (DSC) results showed that as the intercalation reaction progressed, more poly (ethylene oxide), PEO, chains were intercalated and the area of endotherm corresponding to crystalline PEO was reduced. This result agreed with XRD patterns, which demonstrated the increment of intensity of the PEO-intercalated silicate peak. In addition to XRD, the nanocomposite was characterized by transmission electron microscopy (TEM). Well-dispersed individual silicate layers of thickness 10 Å were embedded in the epoxy matrix. This nanocomposite showed improvement in mechanical properties, barrier properties, heat resistance, and thermal

stability. The conductivity of the melt-intercalated hybrid was much higher and more isotropic than of pure matrix.

Liu *et al.* [33] demonstrated the studied on nylon 6-clay nanocomposites by melt-intercalate process. X-ray diffraction and DSC results showed that the crystal structure and crystallization behaviors of the nanocomposites were different from those of nylon 6. Mechanical and thermal testing showed that the properties of the nanocomposites were superior to nylon 6 in terms of heat-distortion temperature, strength, and modulus without sacrificing their impact strength. This was due to the nanoscale effects and the strong interaction between the nylon 6 matrix and the clay interface, as revealed by X-ray diffraction and transmission electron microscope.

Preparation and mechanical properties of polystyrene-clay hybrid were reported by Hasegawa *et al*. [34]. It was found that silicate layers of clay were delaminated and uniformly dispersed to the nanometer level. The strong moduli of the hybrid materials were higher than those of matrix polymer at all temperatures.

Synthesis and characterization of polyaniline (Pan)–clay nanocomposite with extended chain conformation of polyaniline were presented by Wu *et al.* [35]. The conformation emeraldine salt form of polyaniline was inserted into the layers of montmorillonite clay to produce the hybrid with high conductivity. The results showed that a real nanocomposite was obtained and over 90% of the polyaniline chain was inserted between the layers. It was a single chain with extended-chain conformation owing to the confined environment in the nanometer size gallery.

Chang *et al.* [36] prepared poly(lactic acid) nanocomposites by using the solution intercalation method at different organoclay contents. Two organoclays were

synthesized. One was a montmorillonite modified with hexadecylamine (C16-MMT); the other was a fluorinated-mica modified with hexadecylamine (C16-Mica). The tensilie properties of the C16-Mica hybrids were higher than those of the hybrids containing C16-MMT. The optical translucency was not affected by the organoclay content up to 6 wt%; however, the film containing 8 wt% organoclays were slightly cloudier.

Petrovic *et al.* [37] prepared nanocomposites with different concentrations of nanofiller by adding nanosilica filler to the single-phase polyurethane matrix. A control series was prepared with the same concentrations of micron-size silica. The nanosilica filler was amorphous, giving composites with the polyurethane that were transparent at all concentrations. The nanocomposites displayed higher strength and elongation at break but lower density, modulus, and hardness than the corresponding micron-size silica-filled polyurethanes. Although the nanosilica showed a stronger intercalation with the matrix, there were no dramatic differences in the dielectric behavior between the two series of composites.

Chang *et al*. [38] prepared poly(buthylene terepthalate) (PBT)-MMT nanocomposite by using an *in-situ* interlayer polymerization approach. The PBT nanocomposites were melted spun at different organoclay contents to produce monofilaments. The thermal properties of the layered structures of the hybrids were found to be more stable than those of pure PBT. Moreover, the addition of only a small amount of organoclay was enough to improve the mechanical properties of the PBT hybrid fibers.

Hasegawa *et al.* [39] prepared polypropylene-clay hybrids (PPCHs) by melt blending maleic anhydride modified PP and organophilic clay. In these PPCHs the

silicate layers of the clay were exfoliated and dispersed to the monolayers. The hybridization of the clay in PP was achieved with modified PP with a small amount of maleic anhydride groups. The tensile modulus of the PPCH with 5 wt% clay was 1.9 times higher than that of the matrix resin at 25°C. The dynamic storage moduli (É) of the PPCHs were also higher than those of the modified PP. The É was 2.5 times higher than that of the matrix resin at 60°C.

Polysulfone/organoclay nanocomposites were prepared by Sur *et al.* [40] via solution dispersion techniques. The X-ray and microscopy results demonstrated that at least at some composition, the technique employed was successful in exfoliating and widely dispersing the clay platelets. The other measurements demonstrated considerable improvements in strength a modulus, and in thermal stability.

Li *et al*. [41] prepared poly(ethylene-*co*-vinyl acetate) (EVA)/organoclay nanocomposites via melt intercalation process. Three kinds of organoclays were used to observe their influences on the nanostructure of the EVA hybrids. The effects of the polar interactions between the polymer and the silicate layers of organoclays were also investigated by grafting maleic anhydride onto EVA. It was found that the strong polar interactions between the polymer and the silicate layers of organoclays were critical to the formation of polymer-layered silicate nanocomposites. The results also showed that increasing the mixing temperature was unfavorable to improve the dispersion of organoclays in the EVA matrix.

Okada *et al*. [24] prepared two types of biodegradable resins-based clay nanocomposites polycaprolactone (PCL) and polybutylene succinate (PBS) via the direct melt blending method. Characterization of the nanocomposites showed that intercalated and partially exfoliated structures were generated by the melt blending

method. For the mechanical properties, there were improvements in tensile strength and Young's modulus of the nanocomposites due to the reinforcement of nanoparticles. The rheological behaviors of the nanocomposites were significantly affected by the degree of the dispersion of the organoclay was evaluated from the value of the terminal slope of the storage modulus. In addition, the quantity of the shear necessary for making the nanocomposite for melt intercalation method was estimated from the relationship between the value of the terminal slope of the storage modulus and the applied shear.

Zheng *et al.* [42] prepared gelatin/montmorillonite (MMT) hybrid nanocomposites with unmodified MMT and gelatin aqueous solution. The results indicated that an intercalated or partially exfoliated nanocomposite could be achieved, and the properties of the composite were significantly improved. The thermogravity and thermally decomposed rate decreased obviously. The tensile strength and Young's modulus were improved notably, which varied with MMT content, as well as the pH of gelatin matrix.

The use of octadecylamine modified montmorillonite as substitute of carbon black in natural rubber (NR) compounds was studied by Arroyo *et al.* [43] Rubber with 10 phr of clay and octadecylamine modified montmorillonite were compared with 10 and 40 phr carbon black filler. Vulcametric curves showed that the organoclay and carbon black accelerated the vulcanization reaction, and furthermore, gave rise to a marked increase in the torque, indicating a higher degree of crosslinking as was also confirmed by swelling measurements and DSC. The vulcanization rate and torque value of the organoclay compound were sensibly higher than the carbon black compound even at high contents (40 phr). Mechanical characterization showed the strong reinforcing effect of both filler up to 350% in the strength in relation to natural

rubber. The mechanical properties of NR with 10 phr organoclay were comparable to the compound with 40 phr carbon black. Moreover, the organoclay improved the strength of the NR without hardly any reduction in the elasticity of the material.

As an attempt to develop environmentally friendly polymer hybrids, biodegradable thermoplastic starch (TPS)/clay nanocomposites were prepared through melt intercalation method by Park Hwan-Man *et al*. [44]. Natural montmorillonite (Na^+MMT, CloisiteNa^+) and one organically modified MMT with methyl tallow bis-2-hydroxyethyl ammonium cation located in the silicate gallery (Cloisite30B) were chosen in the nanocomposite preparation. TPS was prepared from natural potato starch by gelatinizing and plasticizing it with water and glycerol. The dispersion of the silicate layers in the TPS hybrids was characterized by wide angle X-ray diffraction (WAXD) and transmission electron microscopy (TEM). It was observed that the TPS/CloisiteNa^+ nanocomposites showed higher tensile strength and thermal stability, better barrier properties to water vapor than the TPS/Cloisite30B nanocomposites as well as the pristine TPS, due to the formation of the intercalated nanostructure. The effects of clay contents on the tensile, dynamic mechanical, and thermal properties as well as the barrier properties of the nanocomposites were investigated.

CHAPTER III

EXPERIMENTAL

3.1 Materials and Equipment

3.1.1 Materials

- Cassava starch was purchased from E.T.C. International trading Co., Ltd. where its specification is presented in Table 3.1.

Table 3.1 Specification of cassava starch

Parameter	Composition
Starch content (%)	min. 85
Moisture (%)	max. 12.50 – 13.00
Ash (ml)	max. 0.2
Pulp (ml)	max. 0.2
pH	5.0 – 7.0
Color (%)	90 white
Viscosity (B.U.)	min. 1.00

Source: The Thai Tapioca Flour Industries Trade Association's Standard.

- Commercial grade montmorillonite clay under trade name of Mac-gel (grade WN-02) was supplied by Thai Nippon Chemical Industry Co., Ltd., Thailand. Table 3.2 provides its chemical compositions and physical properties.

Table 3.2 Chemical compositions and physical properties of Mac-gel (grade WN-02)

Typical chemical analysis (on dry basis at 105°C)	
Composition	Value
SiO_2 (%)	55 – 60
Al_2O_3 (%)	14 – 18
Na_2O (%)	2.4 – 3.2
MgO (%)	2.0 – 2.6
CaO (%)	2.0 – 2.5
Fe_2O_3 (%)	1 – 3
K_2O (%)	0.4 – 0.6
TiO_2 (%)	0.2 – 0.3
LOI[a] (%)	10 – 12

[a] **loss on ignition values (LOI) reflect all organic species and all volatiles including moisture.**

Physical Properties

Parameter	Properties
Moisture content (%)	8 – 12
pH value (5% suspension)	9.5 – 11.0
Swelling index (ml per 2 g of clay)	15 – 22
Viscometer dial reading at 600 rpm	12 – 20
Dry particle size passing through 200 mesh (%)	min. 75

- An analytical grade of diethanolamine was purchased from Merck, Hohenbrunn, Germany.

- A commercial grade of glycerol was purchased from Merck, Darmstadt, Germany.

- An analytical grade of acetic acid was purchased from BDH, Poole, England.

3.1.2 Equipment

1. IKA® mechanical stirrer, D-38678, Germany.
2. Brookfield viscometer, RVT 111588, USA.
3. Phynix digital micrometer, Surfix, Germany.
4. Zwick universal testing machine, Zwick Z010, Germany.
5. Macbeth UV-Vis spectrophotometer, Color-Eye 7000, Germany.
6. Philips X-ray diffractometer, PW 3710, Japan.
7. JEOL transmission electron microscope, J200CX TEM, Japan.
8. JEOL scanning electron microscope, JSM-5410LV, Japan.

3.2 Procedure

3.2.1 Montmorillonite/diethanolamine ratio determination

The determination of ion exchange capacity of the montmorillonite was undertaken by the viscosity measurement. The montmorillonite was treated with various amounts of diethanolamine in a range of 0–8 grams dispersed in 150 ml of distilled water, taken into the reactor and stirred at 60°C for 1 hour. A set of various amount of pH with acetic acid was added into montmorillonite dispersion. The mixture

was further stirred at 600 rpm for 10 minutes to allow the complete ion exchange reaction before testing.

3.2.2 Preparation of cassava starch/montmorillonite nanocomposite film

Cassava starch/montmorilonite nanocomposite films were prepared by casting technique. The gelatinized starch solution containing well-dispersed nanoparticles of exfoliated montmorillonite was prepared by mixing 5 grams of oven dried cassava starch with various weight ratio of clay and 1 gram of glycerol. Distilled water was then added to obtain 5wt% starch dispersion. Diethanolamine was added into dispersion. The weight ratio of montmorillonite to diethanolamine in the dispersion was kept at 2:1 which was calculated from the optimum cation exchange capacity value obtained in section 3.2.1. Diethanolamine was converted to cation by the addition of acetic acid. The dispersion was mechanically stirred at 1000 rpm and heated to the gelatinized temperature of starch (70–80°C). The starch solution was cast onto acrylic sheet mold with a wet thickness of 2–3 mm. The cast film was dried overnight at ambient temperature. After the water completely evaporated, films were removed. The schematical diagram for cassava starch/montmorillonite nanocomposite film preparation was shown in Figure 3.1. 5 grams of cassava starch, 1 gram of glycerol, and 95 cm^3 of distilled water were used in every formula with various amounts of montmorillonite (MMT), diethanolamine (DEA), and acetic acid as presented in Table 3.3.

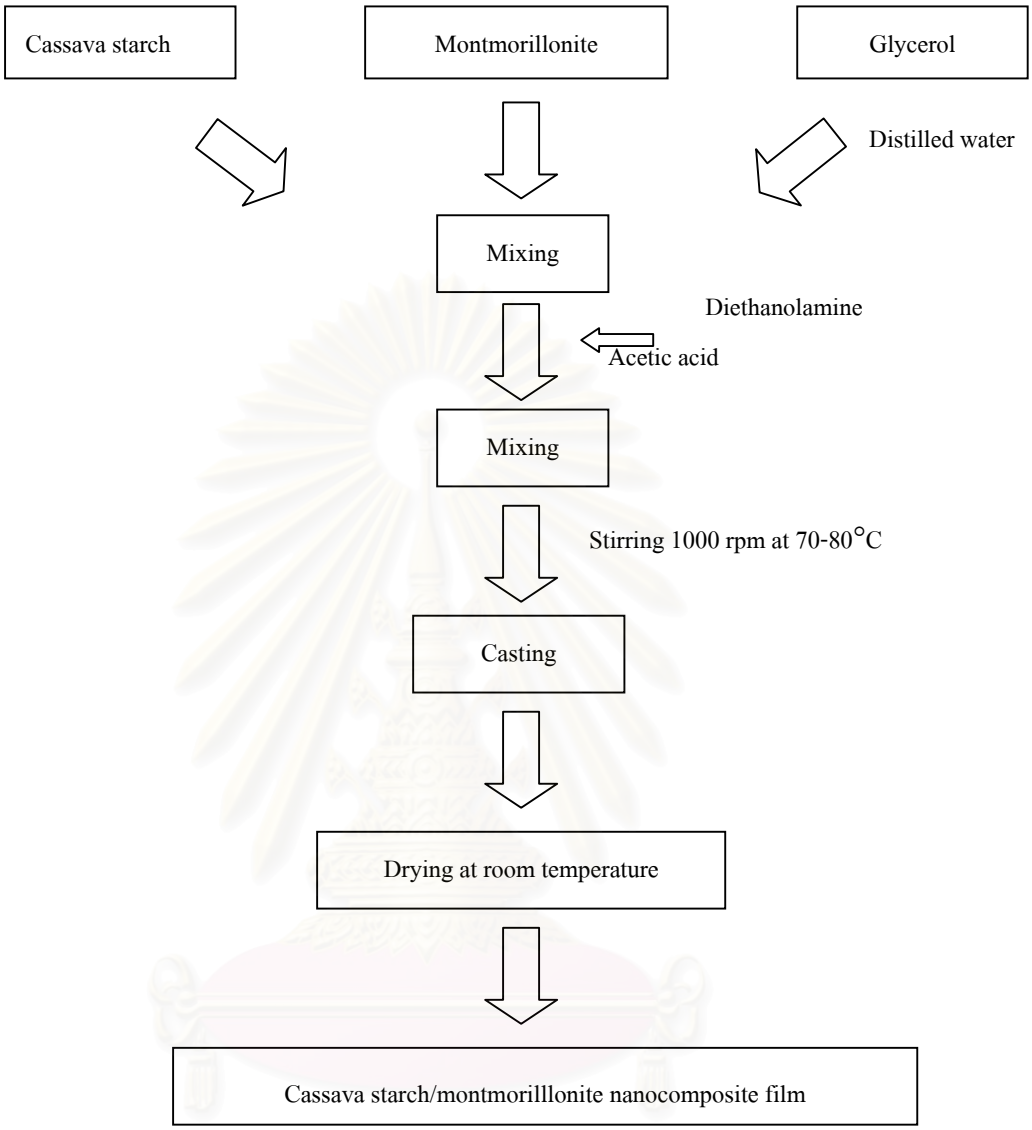

Figure 3.1 The schematical diagram of cassava starch/montmorillonite nanocomposite film preparation.

Table 3.3 The composition of each formula

Formula	Sample code	MMT weight percent (based on starch)	DEA weight percent (based on starch)	Acetic acid weight percent (based on starch)
1	St-C0,D0	–	–	–
2	St-C2,D1	2.0	1.0	0.6
3	St-C4,D2	4.0	2.0	1.2
4	St-C6,D3	6.0	3.0	1.8
5	St-C8,D4	8.0	4.0	2.2
6	St-C10,D5	10.0	5.0	2.8
7	St-C12,D6	12.0	6.0	3.4
8	St-C0,D1	–	1.0	0.6
9	St-C0,D2	–	2.0	1.2
10	St-C0,D3	–	3.0	1.8
11	St-C0,D4	–	4.0	2.2
12	St-C0,D5	–	5.0	2.8
13	St-C0,D6	–	6.0	3.4
14	St-C2,D0	2.0	–	–
15	St-C4,D0	4.0	–	–
16	St-C6,D0	6.0	–	–
17	St-C8,D0	8.0	–	–
18	St-C10,D0	10.0	–	–
19	St-C12,D0	12.0	–	–

3.2.3 Preparation of organoclay for characterization

Twenty grams of montmorillonite clay were added into 800 ml of distilled water. The mixture was well mechanically stirred to obtain the dispersion. Diethanolamine neutralized with acetic acid was added to the clay suspension in a weight ratio equivalent to the cation exchange capacity of the clay (determined in section 3.2.1). The ion exchange reaction was equilibrated for 10 minutes at 60°C. The

supernatant was discarded. The slurry was filtered and washed with distilled water. The collected organoclay was dried at ambient temperature. The schematical diagram of organophilic clay preparation was shown in Figure 3.2

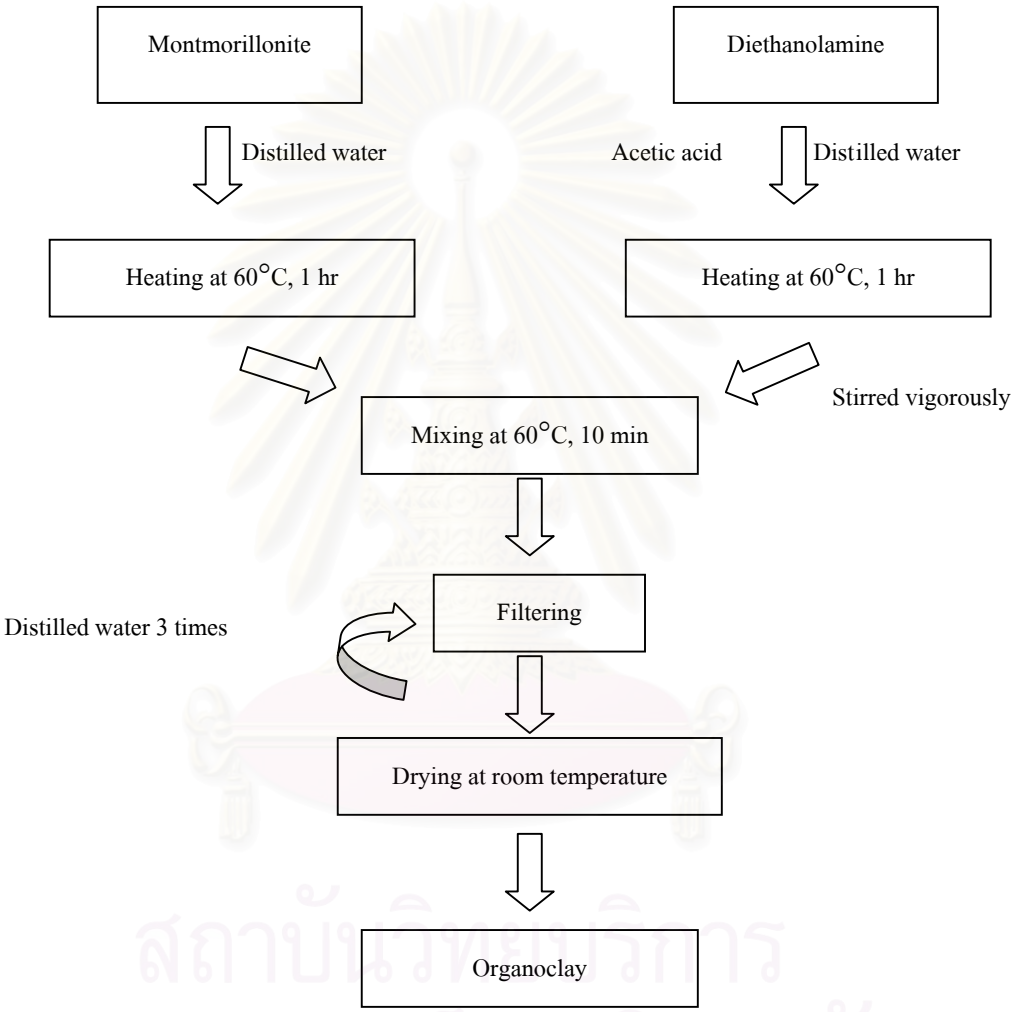

Figure 3.2 The schematical diagram of organoclay preparation.

Characterization

3.3.1 Viscosity

Viscosity of montmorillonite dispersion was measured by Brookfield viscometer model RVT 111588 as shown in Figure 3.3. For each solution (from section 3.2.1), five specimens were tested for each determination.

Figure 3.3 Brookfield viscometer.

3.3.2 X-ray diffraction (XRD)

X-ray diffraction measurements were made directly from montmorillonite and organoclay powders, and nanocomposite film. The test was performed using a PW 3710 Philips diffractometer (Figure 3.6) with CuK_{α} radiation (λ = 0.1542 nm) in sealed tube operated at 40 kV and 30 mA. The diffraction curves were obtained from 2 to 30° at a scanning rate of $1°min^{-1}$.

Figure 3.4 PW 3710 Philips X-ray diffractometer.

3.3.3 Transmission electron microscopy (TEM)

All cassava starch/montmorillonite nanocomposite solution samples were diluted with distilled water (nanocomposite solution: distilled water ratio = 1:20). 300-mesh Cu grids were dipped in these solutions and dried at ambient temperature. TEM images of films were obtained with J200CX TEM shown in Figure 3.7, using an acceleration voltage of 100 kV. High-magnification images were taken at 30,000 and 85,000 times of the original specimens size. Several images of various magnifications over two to three sections per grid were taken to ensure that analysis was based on a representative region of the sample.

Figure 3.5 JEOL J200CX transmission electron microscope.

3.3.4 Scanning electron microscopy (SEM)

The SEM samples were cut from nanocomposite and conventional composite plates. The samples were mounted on stub with double-sided adhesive tape and coated with a thin layer of gold. Images were taken using a JEOL scanning electron microscope, JSM-5410LV as shown in Figure 3.8, using an accelerating voltage of 15 kV, and a magnification 350 times of original specimens size.

Figure 3.6 JEOL JSM-5410LV scanning electron microscope.

3.3.5 Thickness

The thickness of dried film was measured using a Phynix digital micrometer as shown in Figure 3.4. An average of fifteen points was taken for each cassava starch/montmorillonite nanocomposite film.

Figure 3.7 Phynix digital micrometer.

3.3.6 Tensile properties

The tensile strength, % elongation, and modulus values were investigated using Zwick Z010 universal testing machine (Figure 3.5) according to ASTM D882 standard [45]. Samples were cut to 200×15 mm in dimension, and conditioned at 50 ±5%RH, 23 ± 2°C for 24 hours. The gauge length and crosshead speed were 100 mm and 10 mm/min, respectively. The tests were carried out at 23 ± 2°C and 50 ± 5%RH. Each determination was taken from average of five specimens.

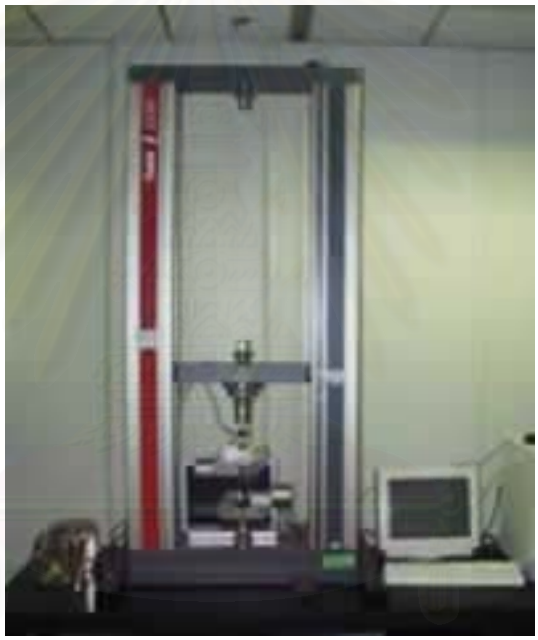

Figure 3.8 Zwick Z010 universal testing machine.

3.3.7 Transparency

Transparency of cassava starch/montmorillonite nanocomposite film was obtained on Instrument Color System (I.C.S.), Macbeth UV-Vis spectrophotometer, mode transmittance at wavelength from 360 to 750 nm. Macbeth UV-Vis spectrophotometer was shown in Figure 3.9.

Figure 3.9 Macbeth UV-Vis spectrophotometer.

3.3.8 Moisture absorption

The moisture absorption of cassava starch/montmorillonite nanocomposite film was determined, and the test specimens were prepared in the dimension of 76.2×25.4 mm. The test specimens were dried in a 50°C oven for 24 hours, then cooled in a desiccator, and immediately weighed to get the initial weight. The specimens were conditioned in a desiccator at 100% RH for 24 hours. After 24 hours, the specimens were removed from the desiccator, dried by wiping with cloth, and the specimens were weighed immediately to obtain the final weight. The percentage of increase in sample weight was calculated by using the below formula.

$$moisture\ \ absorption\ \ (\%) = \frac{final\ \ weight - initial\ \ weight}{initial\ \ \ weight} \times 100 \qquad (3\text{-}1)$$

3.3.9 Water vapor transmission rate (WVTR)

The water vapor transmission rate of cassava starch/montmorillonite nanocomposite film was carried out according to the specification of ISO2528-1995E [46]. A minimum of three 90 mm diameter circular test specimens was prepared from each film sample. The test specimen was fastened to a deep dish containing 15 mm of distilled water using a condition B (temperature 38 ± 1°C and relative humidity 90 ± 2%). The dishes were weighed every hour. The total mass increase graphically as a function of time of exposure, the test being completed when three or four points lie on a straight line. The WVTR for each test piece was then calculated, in grams per square meter per 24 hours, from the equation.

$$WVTR = \frac{240 \times m_1}{S} \tag{3-2}$$

where

m_1 is the rate of increase in mass, in milligrams per hour, determined from the graph.

S is the area, known to within 1%, in square centimeters (normally 50 cm^2), of the tested surface of the test piece.

CHAPTER IV

RESULTS AND DISCUSSION

This project is focused on the development of bioplastic film based on cassava starch. Typically, the disadvantages of starch films are their high degree of water uptake due to the high hydrophilicity of starches. This sensitivity of starch products can be decreased by a homogeneous incorporation of sheet-like non-permeable barrier element such as functionalized layered silicates (clay minerals). In addition, this barrier element sometimes acts as reinforcement filler enhancing the mechanical properties. In order to produce starch film with homogeneous dispersion of nanosized clay platelets, an intercalating agent in this study was diethanolamine (in cationic form by the addition of acetic acid) which was used to exfoliate parallel layers of silicate clay into individual platelets. Prior to the exfoliation occurrence, the intercalating agent underwent cationic exchange reaction with cations on clay surface resulting in the expansion of clay gallery. This phenomenon could notably be observed by the significant increase in the system viscosity. Therefore, a preliminary study was to measure viscosity as a function of the intercalating agent concentration to determine the maximum cation exchange capacity.

4.1 Viscosity

The montmorillonite suspension was treated with diethanolamine in cationic form ($NH[CH_2CH_2OH]_2$) in weight ratios of montmorillonite to diethanolamine varying from 10:0 ─ 10:8. The measured viscosity expressed in centipoises (cps) was recorded and the results are shown in Table 4.1 and graphically illustrated in Figure 4.1.

Table 4.1 Effect of diethanolamine content on the viscosity (cps) of montmorillonite dispersion

MMT:DEA (w/w)	Viscosity (cps)
10:0.0	266 ± 4
10:0.5	1410 ± 14
10:1.0	2300 ± 45
10:2.0	4710 ± 55
10:3.0	5740 ± 55
10:4.0	6040 ± 42
10:5.0	6540 ± 114
10:6.0	6600 ± 71
10:7.0	6520 ± 110
10:8.0	6620 ± 84

It can be seen that viscosity of diethanolamine treated montmorillonite increases rapidly from 10:0 to 10:3, then increases gradually from 10:3 to 10:5, and tends to be constant from 10:5 onward. Change in viscosity was attributed to the cation exchange reaction as explained by reaction shown in Figure 4.2. Before the exchange reaction took place, the stacking parallel platelets of negatively charged layered silicates held together by small cations such as sodium ion (Na^{+}) and calcium ion (Ca^{2+}). When cation exchangeable species as positively charged diethanolamine was replaced into gallery of montmorillonite, basal spacing of montmorillonite was expanded. At the optimum viscosity, the ratio between montmorillonite and diethanolamine was then calculated to determine the maximum cation exchange capacity, which was found to be 2:1. This ratio was then used throughout the experiment for the preparation of starch/montmorillonite nanocomposite film.

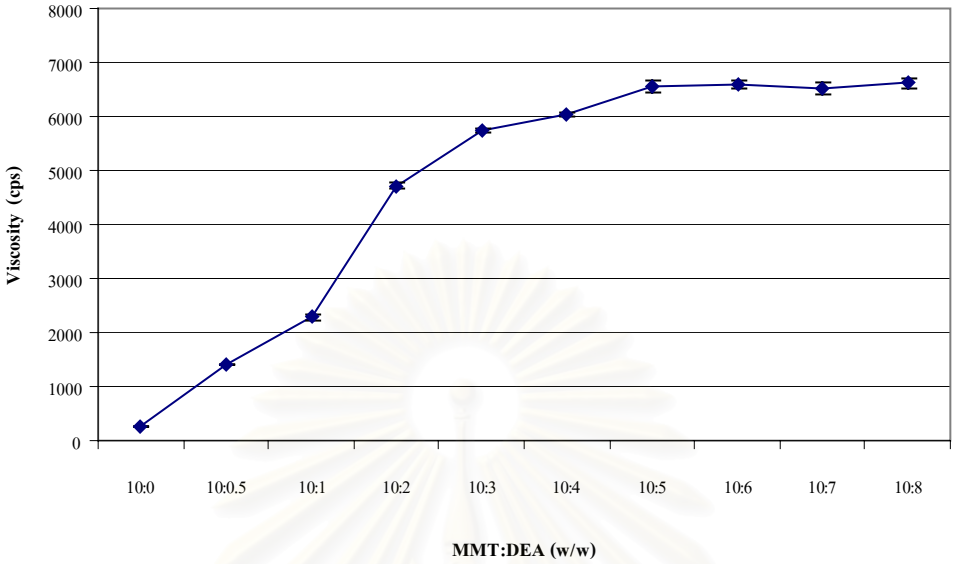

Figure 4.1 The viscosity of montmorillonite dispersion at various amount of diethanolamine.

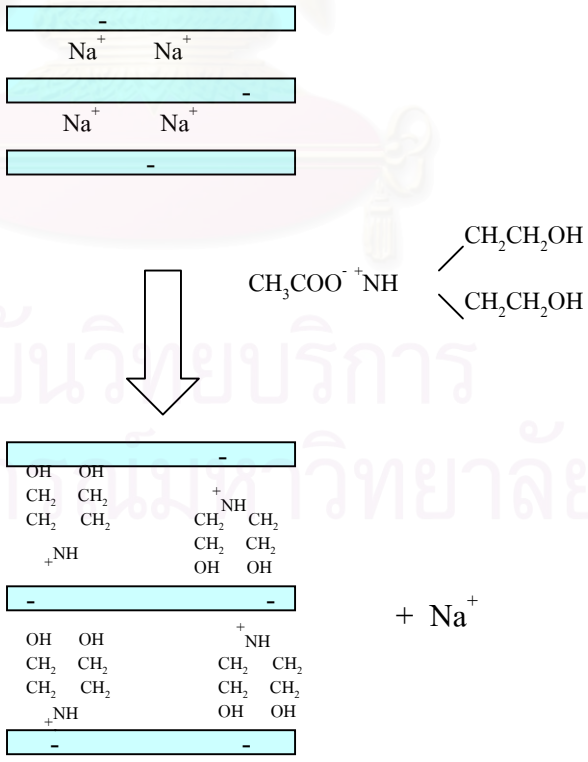

Figure 4.2 A schematic illustration of polymer-clay hybrids.

4.2 X-ray diffraction (XRD)

X-ray diffraction (XRD) is an effective method for the evaluation of the intercalation existence of montmorillonite in polymer matrix. It was expected that the dispersion of montmorillonite in starch nanocomposite existed in two structures: intercalated and exfoliated forms. In case of intercalated nanocomposite, the diffraction peaks shift toward lower diffraction angles indicating that polymer has entered the gallery, expanding the layers, whereas in exfoliated nanocomposites show no diffraction peaks suggesting that a great amount of polymer has entered the gallery space, expanding the clay layers so far apart that diffraction cannot be observed with XRD techniques [47]. In general, larger interlayer spacing has an advantage in the intercalation of polymer chains. It leads to easier dissociation of the clay, which results in hybrids with better dispersions of the clay.

The interlamellar distance can be determined by the diffraction peak and the position of d_{001} in the X-ray technique. The value calculated by Bragg equation is shown below:

$$d_{001} = \frac{\lambda}{2\sin\theta} \tag{4-1}$$

where d_{001} is the interlamellar distance of (001) diffraction face,

θ is the diffraction position,

λ is the wavelength

The wide angle X-ray diffraction (XRD) patterns of montmorillonite (MMT) and diethanolamine modified montmorillonite (MMT-DEA) in the region between $2\theta = 2°$ and $2\theta = 20°$ are shown in Figure 4.3 (a) and (b), respectively. Each curve shows only

one peak at 2θ = 5.975° for MMT and 2θ = 5.590° for MMT-DEA. The peaks assigned to the 001 lattice spacing of silicate layer in montmorillonite as suggested by Usuki *et al*.[48]. The interlayer spacing corresponding of these peaks increases from 14.78 Å to 15.80 Å. In general, the higher degree of basal spacing expansion usually results in the higher chance of polymer intercalation which leads to the more possibility of layered-silicate delamination in the polymer matrix.

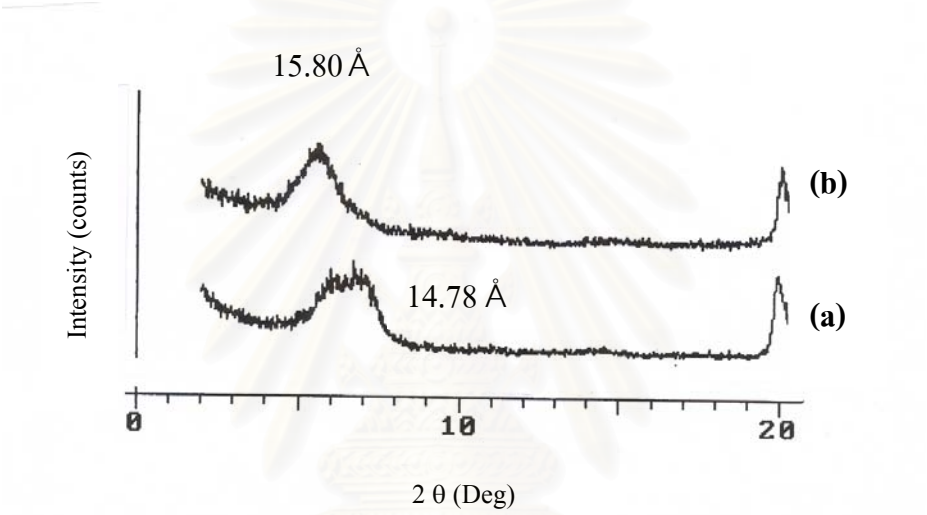

Figure 4.3 XRD patterns of (a) montmorillonite (MMT) and (b) montmorillonite-diethanolamine (MMT-DEA).

Figure 4.4 (a) and (b) shows the XRD pattern of cassava starch film and its clay nanocomposite film. Both films display a broad band in the region between 2θ = 15° and 2θ = 30°. The broad bands indicate that the films contain amorphous regions or partially ordered structures. The XRD pattern of the nanocomposite film also shows a peak at 2θ = 5.015°. The interlayer spacing corresponding of this peak increases up to 17.62 Å. An increase in the interlayer spacing from 15.80 Å in the organoclay to 17.62 Å in the nanocomposite film resulted from some intercalation occurring during the component blending above gelatinize temperature of cassava starch.

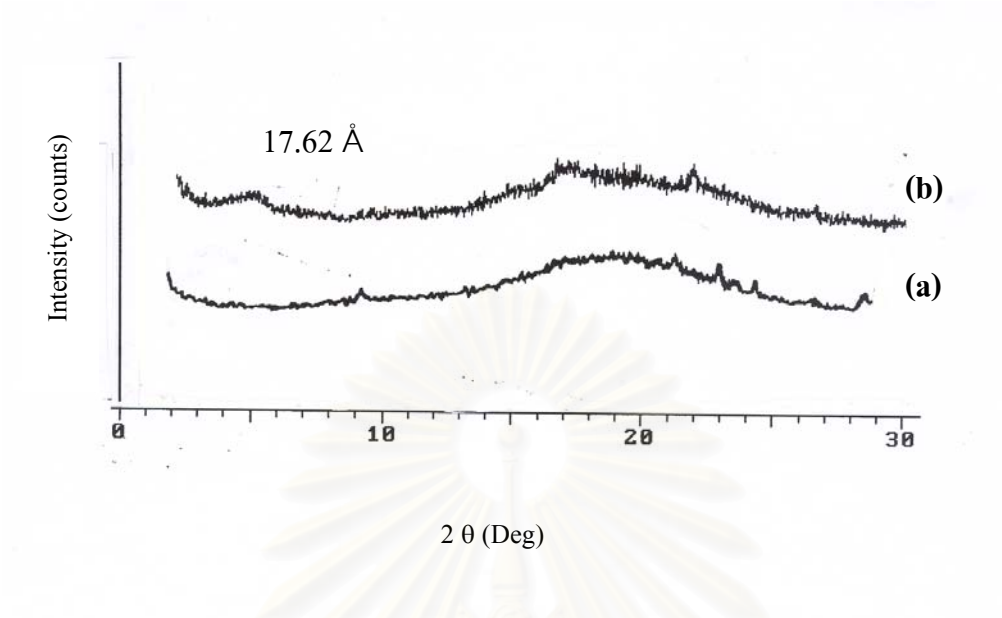

Figure 4.4 XRD patterns of films: (a) cassava starch film and (b) cassava starch/monmorillonite nanocomposite film at 4 wt%.

The XRD results provided the first sign as to the nature of the nanocomposites. Since the formation of an exfoliated structure usually results in complete loss of registry between the clay layers, no peak was observed in the XRD pattern. It is well known that XRD information alone is not sufficient to characterize a nanocomposite. The XRD results noted above gave useful information on the state of the nanocomposites, but did not provide a complete picture. Thus, electron microscopic measurements were required.

4.3 Transmission electron microscopy (TEM)

Changes in interlayer spacing of montmorillonite were confirmed by transmission electron microscopy. Figure 4.5 shows transmission electron micrographs of starch films containing pristine montmorillonite and diethanolamine modified montmorillonite.

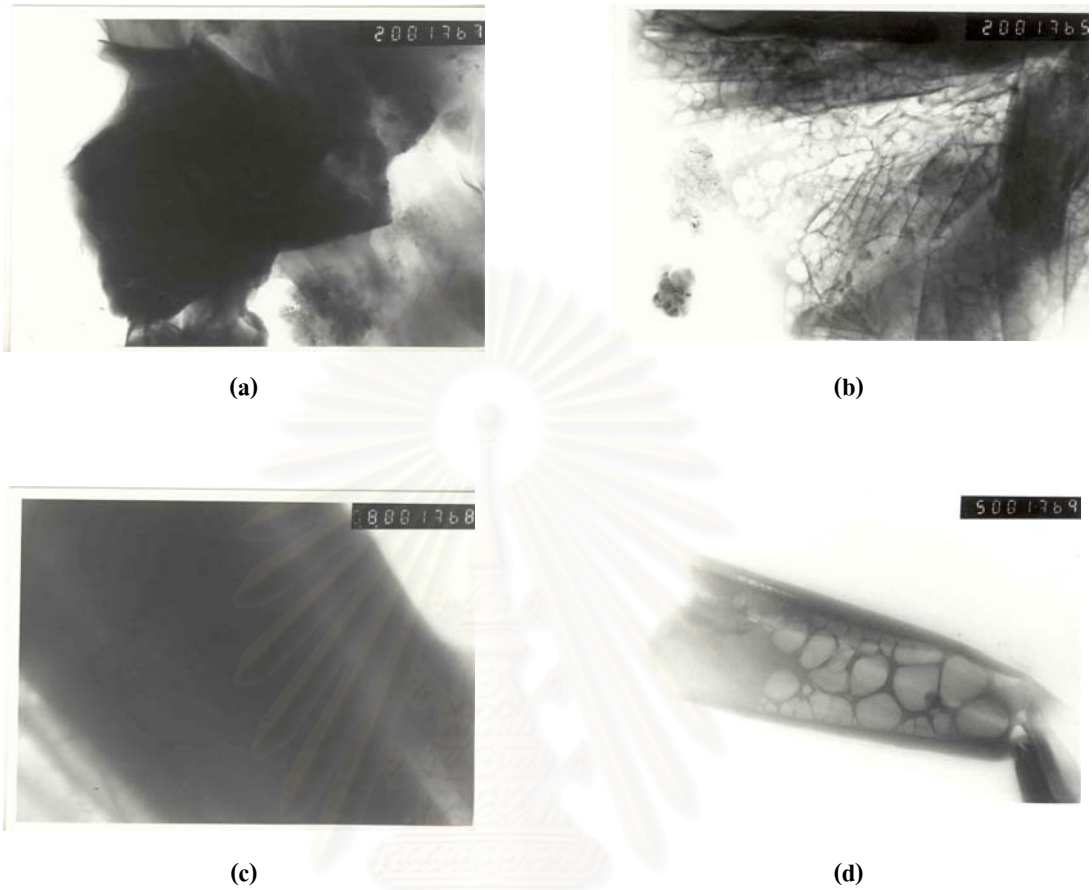

Figure 4.5 TEM photographs of cassava starch/montmorillonite nanocomposite films pristine montmorillonite at (a) 30,000 magnification (c) 85,000 magnification diethanolamine modified montmrillonite at (b) 30,000 magnification (d) 85,000 magnification.

In the case of starch film containing pristine montmorillonite (Figure 4.5 (a) and (c)), no change in interspacing was observed. The clay morphology remained similar to the original structure as shown in Figure 4.6. This result indicated that there was no intercalation taking place with pristine montmorillonite due to the absence of cationic exchangeable species. On the other hand, starch films containing diethanolamine modified montmorillonite in Figure 4.5 (b) and (d) shows the individual alumino-

silicate layers. The clay morphology was so different from the pristine montmorillonite. These results showed the existence of intercalated pattern of the clay because diethanolamine is exchangeable cationic species which were consistent with the XRD pattern. However, the silicate layers have very strong electrostatic interactions between silicate layers through intergallery cations make it extremely difficult to achieve complete exfoliation of the layers.

Figure 4.6 TEM micrograph of montmorillonite at 140,000 magnification by Wang *et al.* [25].

4.4 Scanning electron microscopy (SEM)

The scanning electron micrographs of starch/montmorillonite nanocomposite film were measured by JEOL scanning electron microscope. Comparison between a nanocomposite and a conventional composite structure was shown in Figure 4.7. The bright spots on images correspond to clay aggregates. Figure 4.7 (a) presents the microstructure of a nanocomposite with diethanolamine modified montmorillonite

4wt%. The clay particles were finely dispersed in the material. In the conventional composite (Figure 4.7(b)), large aggregates around 10 μm in the diameter were observed. Apparently, the clay particles were more finely dispersed in the nanocomposite as compared with the conventional composite. The difference may be due to the treatment of the clay. The hydroxylammonium ions render the clay organophilic and allow a better dispersion of the clay in an organic medium. Small particle aggregates were observable at relatively low magnification.

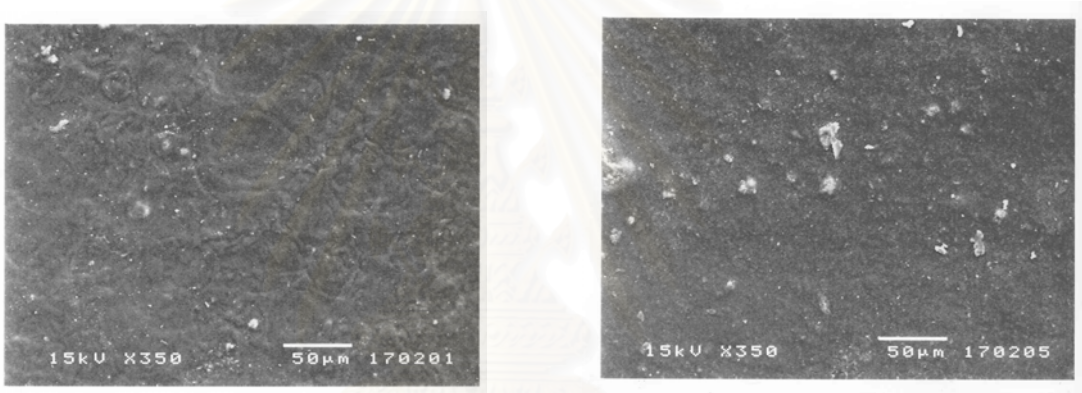

(a) **(b)**

Figure 4.7 SEM micrographs of cassava starch/montmorillonite nanocomposite films at MMT 4wt% (a) diethanolamine modified montmorillonite (b) pristine montmorillonite.

4.5 Thickness measurement of starch/montmorillonite nanocomposite film

In this study, series of starch films containing various amounts of montmorillonite were prepared. It was possible that varying amounts of clay might affect the film thickness and consequent the mechanical properties. Film thickness measurement was, therefore, carried out using Phynix digital micrometer. As shown in Table 4.2, film thickness of each film formula was measured to be approximately 71

microns. These results indicated that dry film thickness was not significantly varied with different amount of added clay. The mechanical properties of film therefore were reasonably comparable.

Table 4.2 Thickness of cassava starch/montmorillonite nanocomposite films

Formula	Thickness (μm)
St-C0, D0	71.2 ± 4.09
St-C2, D1	71.4 ± 3.14
St-C4, D2	71.3 ± 2.67
St-C6, D3	71.3 ± 2.96
St-C8, D4	71.7 ± 4.14
St-C10, D5	71.4 ± 3.42
St-C12, D6	71.6 ± 3.73

4.6 Tensile properties of starch/montmorillonite nanocomposite film

The mechanical properties of starch/montmorillonite nanocomposite film were measured using Zwick universal testing machine. The tensile properties of film samples were measured in terms of tensile strength, % elongation at break, and Young's modulus according to ASTM D 882. The results are given in Table 4.3.

Table 4.3 Average of tensile properties of various films at various MMT and DEA contents

Formula	MMT,DEA weight percent (based on starch)	Tensile strength (MPa)	Elongation at break (%)	Young's Modulus (MPa)
St-C0, D0	0,0	18.52 ± 0.37	4.53 ± 0.63	748.58 ± 8.28
St-C2, D0	2,0	18.64 ± 0.35	4.12 ± 0.34	755.11 ± 11.29
St-C4, D0	4,0	19.13 ± 0.29	3.88 ± 0.26	761.08 ± 6.55
St-C6, D0	6,0	19.51 ± 0.50	3.86 ± 0.32	762.72 ± 4.74
St-C8, D0	8,0	19.05 ± 0.65	3.74 ± 0.31	757.24 ± 6.41
St-C10, D0	10,0	18.96 ± 0.88	3.35 ± 0.20	757.55 ± 10.57
St-C12, D0	12,0	18.42 ± 0.49	3.27 ± 0.16	755.45 ± 5.11
St-C0, D1	0,1	10.66 ± 0.45	9.49 ± 0.57	464.36 ± 5.71
St-C0, D2	0,2	10.06 ± 0.41	13.16 ± 1.20	405.91 ± 10.21
St-C0, D3	0,3	8.06 ± 0.21	23.10 ± 1.19	252.12 ± 5.92
St-C0, D4	0,4	5.66 ± 0.28	31.91 ± 1.59	157.84 ± 8.00
St-C0, D5	0,5	5.18 ± 0.18	40.62 ± 1.23	138.86 ± 6.49
St-C0, D6	0,6	4.18 ± 0.14	46.47 ± 1.22	86.10 ± 2.41
St-C2, D1	2,1	12.55 ± 0.25	7.10 ± 0.61	537.24 ± 11.91
St-C4, D2	4,2	11.47 ± 0.93	10.51 ± 1.60	441.15 ± 10.22
St-C6, D3	6,3	9.14 ± 0.85	18.49 ± 0.63	392.24 ± 8.29
St-C8, D4	8,4	5.50 ± 0.34	27.45 ± 0.68	205.31 ± 7.55
St-C10, D5	10,5	5.05 ± 0.22	34.27 ± 2.27	151.78 ± 4.85
St-C12, D6	12,6	4.80 ± 0.44	43.14 ± 1.26	107.52 ± 6.25

According to the viscosity measurement, the ratio 2:1 of MMT:DEA was applied for all the tensile properties by varying the amount from 0,0 to 12,6 w/w of starch. Furthermore, in this work the tensile properties of nanocomposite films contained MMT,DEA compared with their no MMT and no DEA were investigated.

Figures 4.8 and 4.9 show tensile strengths and Young's modulus of the films. From Figure 4.8 and 4.9, starch film containing various amounts of pristine montmorillonite exhibits insignificant difference in tensile strength and Young's modulus. The addition of montmorillonite brought about slight increasing in tensile strength and Young's modulus. The ineffective reinforcement of the clay particle probably was due to the phase separation between starch matrix and clay filler.

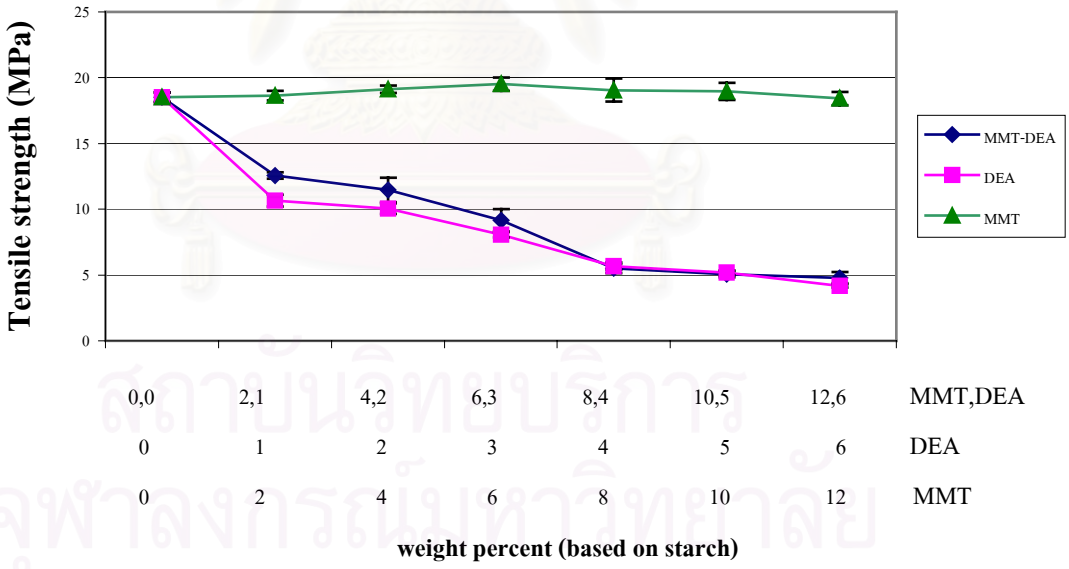

Figure 4.8 Tensile strength of nanocomposite films.

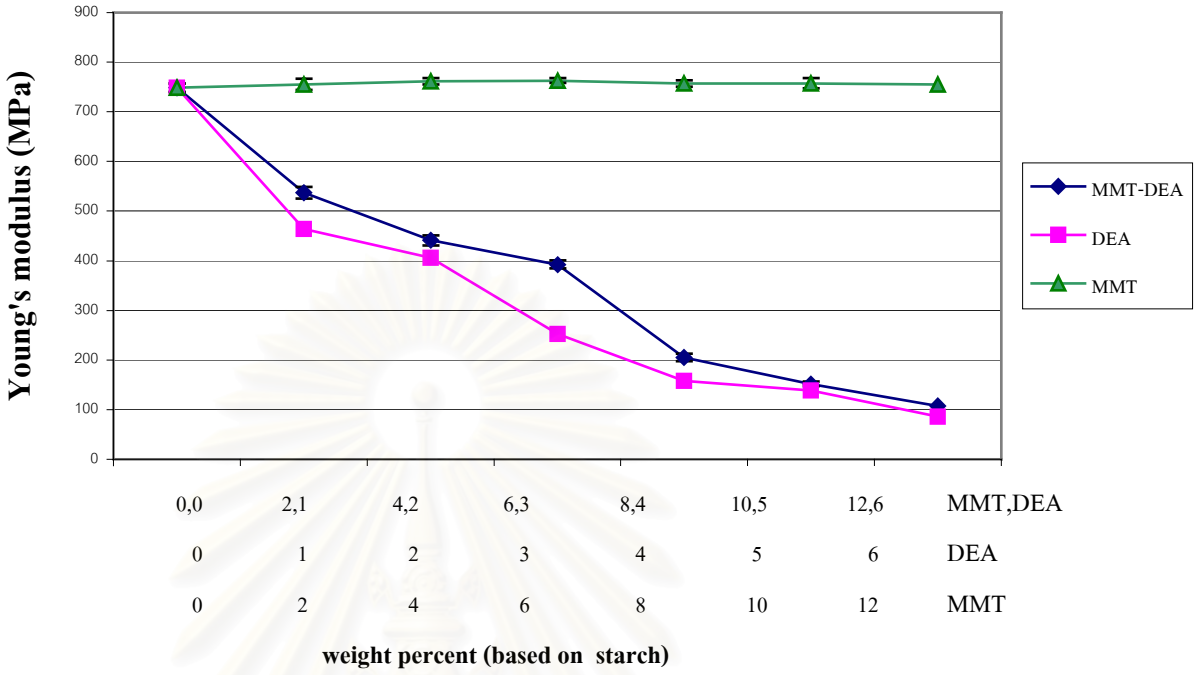

Figure 4.9 Young's modulus of nanocomposite films.

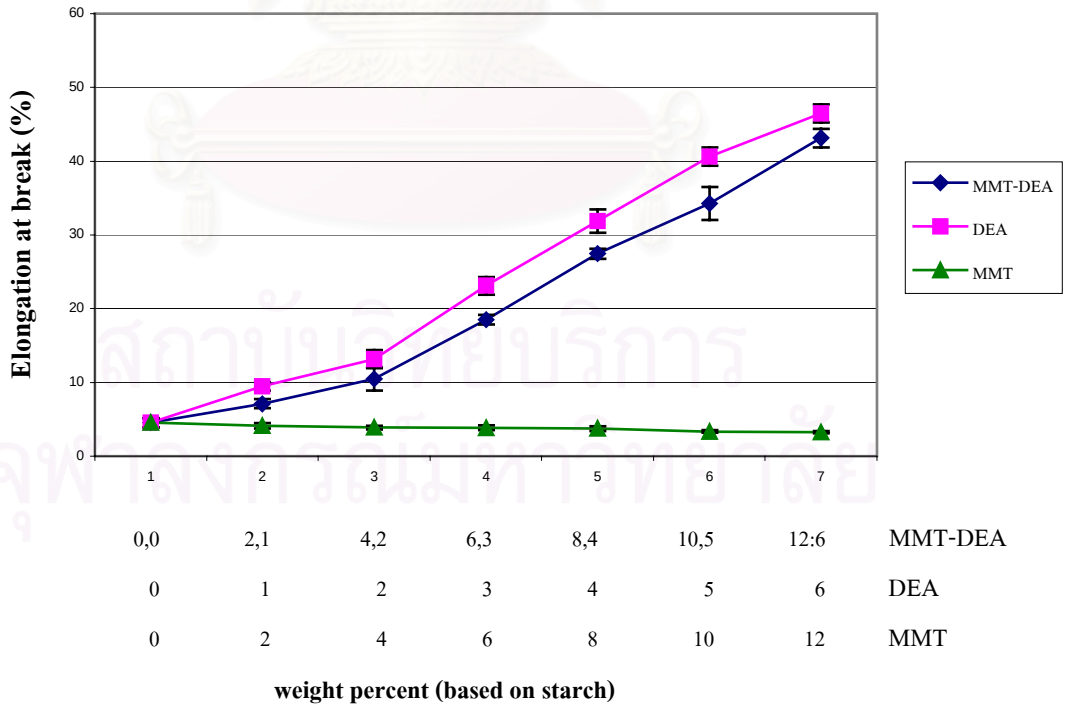

Figure 4.10 Elongation at break of nanocomposite films.

In the case of intercalated montmorillonite, it was generally expected that increase in tensile strength and Young's modulus should be observed by largely increased surface area of montmorillonite due to the intercalation by DEA. However, it was disappointing that the resulting evidence presented in Figures 4.8 and 4.9 were totally opposite. Tensile strength and Young's modulus of nanocomposite film gradually decreased with the increased content of montmorillonite. Furthermore, it can be seen that tensile strength and Young's modulus tended to decrease as MMT,DEA ratio increased, implying that diethanolamine adversely affected the tensile strength and Young's modulus of film. A possible reason for the large decreasing in tensile strength and Young's modulus was due to the hygroscopic nature of DEA. The nanocomposite films were prone to adsorb more moisture, consequently contributing to the plasticizer effect of DEA.

Figures 4.8 and 4.9 show that there is a sharp decrease in tensile strength and Young's modulus as DEA increased from 0 to 6 wt%. In addition, the elongation at breaks of the hybrid films is shown in Figure 4.10. The elongation at breaks of nanocomposite starch was clearly seen to increase with increasing MMT-DEA content. The explanation to this phenomenon based on the fact that diethanolamine behaved like glycerol, which is a typical plasticizer for starch products.

4.7 Transparency

Film transparency which relates to the ability of light passing through is one of indicators that provide the information of particle size of dispersed particle in starch matrix. The particle sizes larger than the visible wavelength would obstruct light, hence leading to translucent or opaque film. Transparency of nanocomposite film was

expressed as percent transmittance measured using UV/VIS spectrophotometer. Figure 4.11 compared the percent transmittances of starch/montmorillonite nanocomposite films including MMT,DEA and MMT over the wavelength of 360-750 nm. From the Figure 4.11, the plain starch film due to the absence of light blockage particles exhibits the highest percent transmittance followed by the starch/montmorillonite nanocomposite film and starch film containing pristine montmorillonite, respectively. The difference in transmittance values of starch/montmorillonite nanocomposite film and starch/pristine montmorillonite film was believed to be related to the different sizes of the dispersed particles.

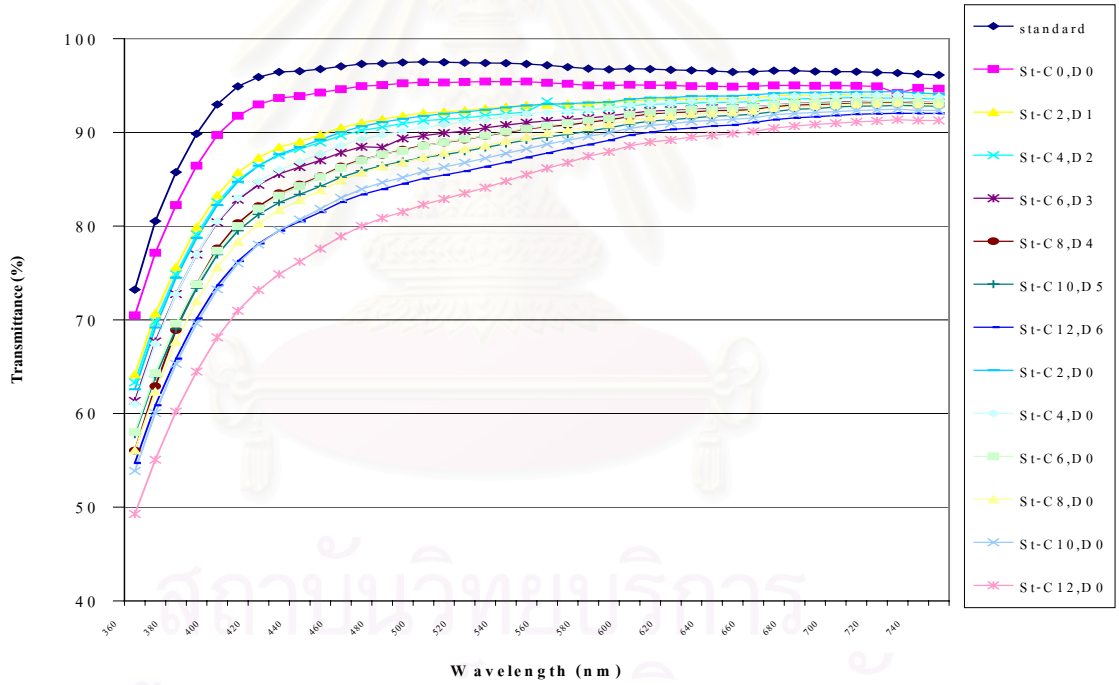

Figure 4.11 Transparency of starch film and nanocomposite film.

Figure 4.12 compares the percent transmittance valuesof films at fixed wavelength of 500 nm. It is clearly seen that starch/montmorillonite nanocomposite film exhibited relatively higher transparency, resulting from the smaller disperse phase domain of nanoparticles. The results of transparency measurement also provide an

information that nanoscale dispersion of montmorillonite in starch matrix could be achieved up to the maximum amount of 10 wt% montmorillonite which was defined according to the physical appearance by visual inspection. Further addition above this point resulted in the occurrence of phase separation between starch matrix and clay particle, which reflected in changing trend of percent transmittance.

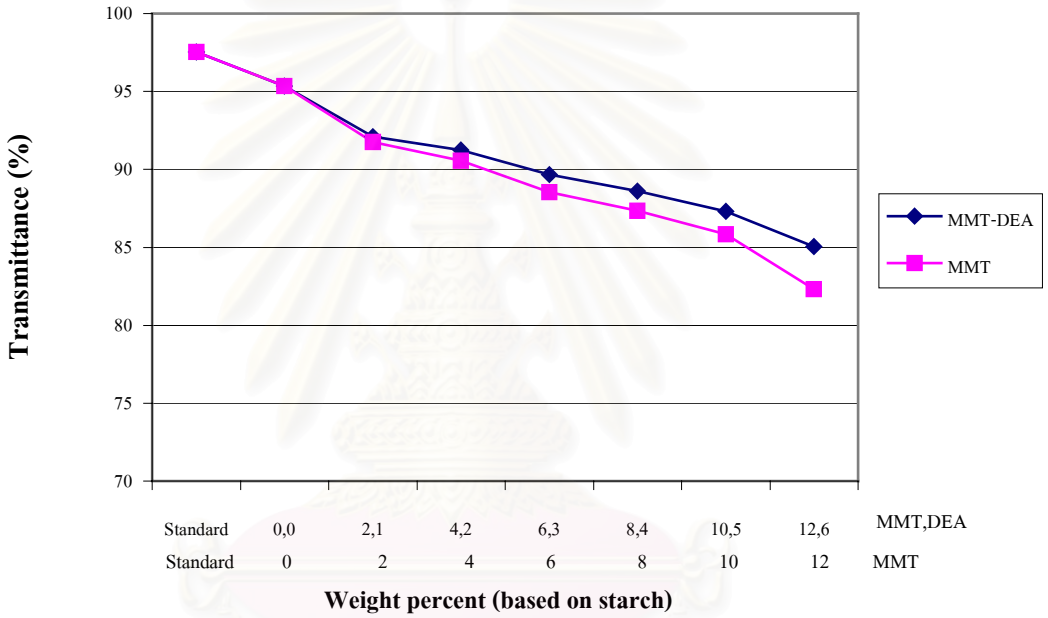

Figure 4.12 Transparency of cassava starch/montmorillonite nanocomposite film at wavelength 500 nm.

4.8 Moisture absorption

The moisture uptake capacity of nanocomposite films was studied. The results are shown in Table 4.4.

Table 4.5 The effect of MMT, DEA content to moisture absorption

Formula	MMT,DEA weight percent (based on starch)	Moisture absorption (%)
St-C0, D0	0,0	135.82 ± 1.17
St-C2, D1	2,1	136.28 ± 2.87
St-C4, D2	4,2	138.37 ± 1.66
St-C6, D3	6,3	138.26 ± 4.76
St-C8, D4	8,4	141.16 ± 3.28
St-C10, D5	10,5	141.29 ± 4.79
St-C12, D6	12,6	142.41 ± 3.47

From Figure 4.13, it can be observed that moisture absorption of nanocomposite film increases gradually with an increase in amount of MMT as well as DEA (since the latter is proportional to MMT content). Therefore, it is no doubt that the moisture uptake capability of the nanocomposite film largely influenced by the presence of DEA due to its hygroscopic nature. However, it was unavoidable to reduce the amount of DEA since optimum intercalation of montmorillonite would be affected. Concerning the properties of packaging films, film hygroscopicity is not desirable It is, therefore, not recommended the use of DEA as an intercalating agent for starch/montmorillonite nanocomposite in the packaging area.

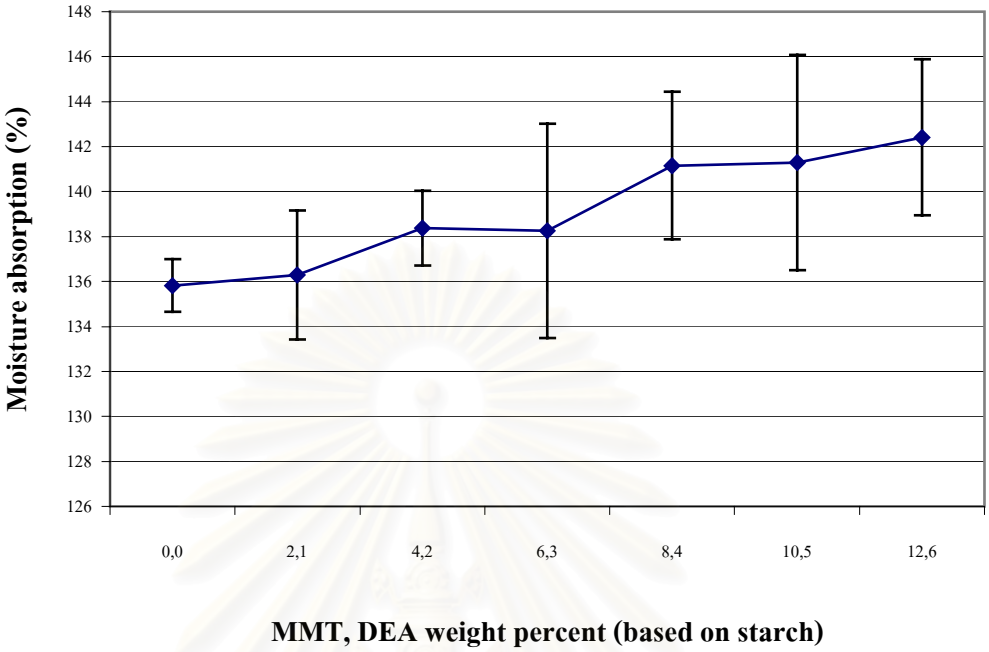

Figure 4.13 Plot of percentages of moisture absorption of nanocomposite films at various formulations.

4.9 Water vapor transmission rate

The average thickness of the nanocomposite film with pristine montmorillonite and diethanolamine modified montmorillonite used for water vapor transmission rate (WVTR) determination was about 70 microns. WVTR values for a 70-micron thickness are given in Table 4.6 and Figure 4.14. Furthermore, the dependence of MMT, DEA content on water vapor transmission rate was also investigated.

Table 4.6 Water vapor transmission rate of cassava starch/montmorillonite nanocomposite film

Formula	MMT,DEA weight percent (based on starch)	Water vapor transmission rate ($g/m^2.day$)
St-C0, D0	0,0	1997.96 ± 95.19
St-C2, D1	2,1	2013.56 ± 103.39
St-C4, D2	4,2	2126.60 ± 191.34
St-C6, D3	6,3	2209.00 ± 101.96
St-C8, D4	8,4	2175.22 ± 175.35
St-C10, D5	10,5	2230.68 ± 216.53
St-C12, D6	12,6	2322.29 ± 113.22

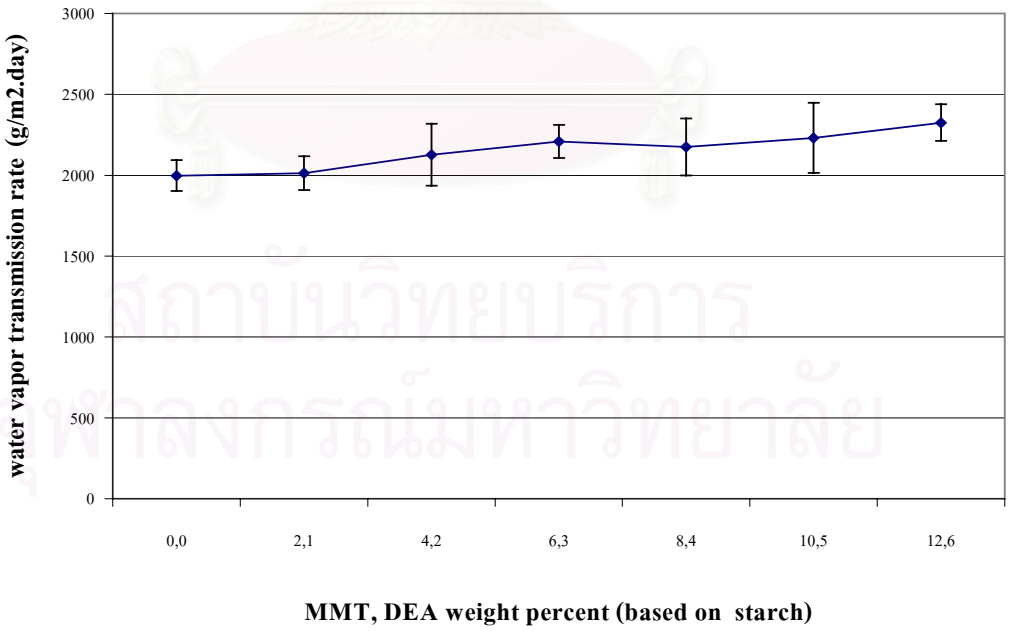

Figure 4.14 Effect of MMT,DEA content on water vapor transmission rate of various films.

The cassava starch/montmorillonite nanocomposite film was found to be superior in its permeability property to ordinary cassava starch film. For nanocomposite films, the results showed that the higher content of MMT,DEA resulting in the higher water vapor transmission rate. The explanation to this phenomenon is based on the fact that diethanolamine is a plasticizer like glycerol. However, it was unavoidable to reduce the amount of DEA since optimum intercalation of montmorilonite would be affected. When the plasticizer content (such as water, glycerol, and diethanolamine) increased in the nanocomposite film, the WVTR increased (Table 4.6). The increase in WVTR could be either attributed to greater interchain distances in the presence of plasticizer or to a denser packing of polymer chains.

CHAPTER V

CONCLUSIONS

5.1 CONCLUSIONS

A starch/clay nanocomposite consisted of montmorillonite at the molecular level has been synthesized by using cassava starch and montmorillonite intercalated with an ammonium salt of diethanolamine. The cation-exchange capacity of the montmorillonite was of importance in the synthesis of cassava starch/montmorillonite nanocomposite films because it determined the amount of alkylammonium ions, which can be intercalated between the layers. In this context, the optimum cation exchange capacity was 2:1 of montmorillonite to diethanolamine ratio.

Both cassava starch and starch/clay nanocomposite films were subsequently prepared by means of solution casting techniques. As seen from XRD patterns and TEM micrographs of nanocomposite film, this hybrid had a special structure in which montmorillonite dispersed homogenously. These results suggested that starch-clay nanocomposite can be classified as intercalated nanocomposite.

On the microscale, SEM micrographs demonstrate a finer dispersion of the clay particles in the nanocomposite as compared with the conventional composites based on the same constituents. The difference may be due to the treatment of the clay which the hydroxylammonium ions render the clay organophilic and allow a better dispersion of the clay in starch matrix.

Tensile strength and Young's modulus of starch/clay nanocomposite films decreased, but their percentage elongation increased with increasing the MMT, DEA contents. The explanation to this phenomenon is based on the fact that diethanolamine is a plasticizer like glycerol.

Films were highly translucent, but the translucency of nanocomposite films slightly decreased with increasing montmorillonite and diethanolamine contents. At the same content, the films that contained prinstine montmorillonite were cloudier than those of diethanolamine modified montmorillonite. The translucency of the hybrids films was due to the degree of clay particle dispersion in the matrix polymer.

Moisture absorption and water vapor transmission rate of nanocomposite films increased with increasing MMT and DEA contents because diethanolamine is a plasticizer for nanocoposite film.

5.2 SUGGESTION

It is suggested that natural intercalating agents such as gelatin, chitosan, and other cationic polymers are recommended to replace diethanolamine (DEA). Particularly, Chitosan may be the most suitable due to compatibility with starch and relative more hydrophobicity.

REFERENCES

1. Wurzburg, D. B. 1998. Modified starches: Properties and uses. Boca Raton. FL: CRC Press.
2. Arvanitoyannis, I., Biliaderis, C. G., Ogawa, H., and Kawasaki, N. 1998. Biodegradable films made from low density polyethylene (LDPE), rice starch, and potato starch for food packaging applications: Part1. Carbohydrate Polymers, 36, 89-104.
3. Psomiadou, E., Arvanitoyannis, I., Biliaderis, C. G., Ogawa, H., and Kawasaki, N. 1997. Biodegradable films made from low density polyethylene (LDPE), wheat starch and soluble starch for food packaging applicants: Part2. Carbohydrate Polymers, 33, 227-242.
4. Fishman, M. L., Coffin, D. R., Konstance, R. P., and Onwulate, C. I. 2000. Extrusion of pectin/starch blends plasticized with glycerol. Carbohydrate Polymers, 41, 317-325.
5. Abdul-Hatiz, S. A. 1997. Synthesis and characterization of hypochlorite oxidized poly(methyacrylic acid)-starch composite. Polymer Degradation and Stability, 55(1), 9-16.
6. Simkovic, N., Laszlo, J. A., Thompson, A. R. 1996. Preparation of a weakly basic ion exchange by crosslinking starch with epichlorohydrin in the presence of NH_4OH. Carbohydrate Polymers, 30(1), 25-30.
7. Kim, J. W., Noh, M. H., Choi. H. J., Lee, D. C., and Jhon, M. 2000. Synthesis and electrorheological characteristics of SAN-clay composite suspensions. Polymer, 41, 317-325.
8. Murray, H. H. 2000. Traditional and new applications for kaolin, smectite and polygorskite: A general overview. Applied Clay Science, 17, 207-221.

9. López-Manchado, M.A., Arroyo, M., Herrero, B., and Biagiotti. 2003. Vulcanization kinetics of natural rubber-organoclay nanocomposites. Journal of Applied Polymer Science, 89, 1-15.

10. Sriroth, K., Piyachomwan, K., Sangseethong, K., and Oates, C. 1999. Modification of cassava starch. [online]. Available from: www.cassava .org /Poland/Modification.pdf. [2003, Nov 12].

11. Sur, G. S., Sun, H.L., Lyu, S. G., and Mark, J. E. 2001. Synthesis, structure, mechanical properties, and thermal stability of some polysulfone/organoclay nanocomposites, Polymer, 42, 9783-9789.

12. Delozier, D.M., Orwell, R.A., Cahoon, J. F., Johnston, N. J., Smith Jr, J.G., and Connell, J.W. 2002. Preparation and characterization of polyimide/organoclay nanocomposites, Polymer, 43, 813-822.

13. Meadows, Cameron. 1998. The effect of aging on biodegradable starch plastic film. B.Sc. Thesis in Engineering, The Department of Chemical Enginnering, The University of Queenland.

14. FAOSTAT: 2002. Cassava processing [online]. Available from: www.fao.org/inpho/vibrary/x0032e/x0032E04.htm [2002, Oct 30]

15. Richard, A. G., and Bhanu, K.: 2002. Biodegradable polymers for the environment [online]. Available from: www.sciencemag.org [2002, Aug 2]

16. Kashiwagi, T., Morgan, A. B., Antonucci, J. M., Vanlandingham, M. R., Harris Jr., R. H., Awad, W. H., and Shields, J. R. 2003. Thermal and flammability properties of a silica-poly (methylmethacrylate) nanocomposite. Journal of Applied Polymer Science, 89, 2072-2078.

17. Charles, E. W., and Lin, D. P. 1975. The chemistry of clay minerals. New York. Elsevier Scientific.

18. Khayankarn, Orasa. 1999. Adhesion and permeability of polyimide-clay nanocomposite as protective coating for microelectronic gas sense. M.S.

Thesis in Polymer Science, The Petroleum and Petrochemical College, Chulalongkorn University.

19. Johnson, J. M. 2000. Lecture 12- Clay minerals Soil Science Division, University of Idaho, Moscow. [online].: Johnson, J. M. 2003. Available from: http://soils.ag.uidaho.edu/soil205-90/Lecture%208/ [2002, Nov 19]

20. Horal, E. 1999. Basic characteristics of engineering soils, Department of Civil and Biosystems Engineering, University of Pretoria. [online]. Available from: http://www.up.ac.za/academic/civil/ [2003, Jan 10]

21. Kornmann, X. 2000. Polymer-layered silicate nanocomposites [online]. Available from: www.instmat.co.uk. [2003, Jan 13].

22. Thaijaroen, Woothichai. 2000. Preparation and mechanical properties of NR/clay nanocomposite. M.S. Thesis in Polymer Science, The Petroleum and Petrochemical College, Chulalongkorn University.

23. Kurt, Jordens. 1999. Hybrid inorganic–organic materials: Novel poly(propylene oxide) based ceramers, abrasion resistant sol–gel coatings for metals, and epoxy–clay nanocomposites. Ph.D. Thesis in Chemical Engineering, Virginia Polytechnic Institute and State University.

24. Okada, K., Mitsunaga, T., and Nagase, Y. 2003. Properties and particles dispersion of biodegradable resin/clay nanocomposite. Korea-Australia Rheology Journal, 15, 43-50.

25. Wang, S., Hu, Y., Tang, U., Wang, Z., Chen, Z., and Fan, W. 2003. Preparation of polyethylene-clay nanocomposites directly from Na^{+} montmorillonite by a melt intercalation method. Journal of Applied Polymer Science, 89, 2583-2585.

26. Abdul, A. S., Gibson, T. L., and Rai, D. N. 1990. Laboratory studies of the flow organic solvents and their aqueous solutions through bentonite and kaolin clay. Ground Materials, 28(4), 524-533.

27. Choy, J. H., Kwak, S. Y., Han, Y. S. and Kim, B. W. 1997. New organo-montmorillonite complexes with hydrophobic and hydrophilic functions. Materials Letters, 33(3-4), 143-147.

28. Yang, R. T. and Cheng, L. S. 1997. Tailoring micropore dimensions in pillared clay for enhanced gas adsorption. Microporous Materials, 8, 177-186.

29. Yano, K., Usuki, A., Okada, A., Kurauchi, T., and Kamigaito, O. 1993. Synthesis and properties of polyimide-clay hybrid. Journal of Polymer Science: PartA: Polymer Chemistry, 31, 2493-2498.

30. Messersmith, P. B., and Giannelis, E. P. J. 1995. Synthesis and barrier properties of poly(ε-caprolactone)-layered silicate nanocomposites. Journal of Polymer Science Part A: Polymer Chemistry, 33, 1047-1057.

31. Pinnavaia, T. J., Lan, T., Wang, Z., Shi, H., and Kaviratna, P. D. 1996. Clay-reinforced epoxy nanocomposites: Synthesis, properties, and mechanism of formation. ACS Symposium Series, 622(17), 250-261.

32. Giannelis, E. P. 1996. Polymer Layered silicate nanocomposites. Advanced Material, 8(1), 29-35.

33. Lui, L., Qi, Z., and Zhu, X. 1999. Studies on nylon6/clay nanocomposites by melt-intercalattion process. Journal of Applied Polymer Science, 71, 1133-1138.

34. Hasegawa, N., Okamoto, H., Kawasumi, M., and Usuki, A. 1999. Preparation and Mechanical properties of polystyrene-clay hybrids. Journal of Applied Polymer Science, 74, 3359-3364.

35. Wu, Q., Xue, Z., Qi, Z., and Wang, F. 2000. Synthesis and characterization of PAn/clay nanocomposite with extended chain conformation of polyaniline. Polymer, 41, 2029-2032.

36. Chang, J. H., An, Y. U., and Sur, G. S. 2002. Poly(lactic acid) nanocomposites with various organoclays. I. Thermomechanical properties, morphology and

gas permeability. Journal of Polymer Science Part B: Polymer Physics, 41(1), 94-103.

37. Petrovic, Z. S., Javni, I., Waddon, A., and Banhegyi, G. 2000. Structure and properties of polyurethane-silica nanocomposites. Journal of Applied Polymer Science, 76, 131-151.

38. Chang, J., An, Y. U., Ryu, S. C., and Giannelis, E. P. 2003. Synthesis of poly(buthylene terephthalat) nanocomposite by *in-situ* interlayer polymerization and characterization of its fiber (I), Polymer Bulletin, 51, 69-75.

39. Hasegawa, N., Okamoto, H., Kato, M., and Usuki, A. 2000. Preparation and mechanical properties of polypropylene-clay hybrids based on modified polypropylene and organophilic Clay. Journal of Applied Polymer Science. 78, 1918-1922.

40. Sur, G. S., Sun, H. L., Lyu, S. G., and Mark, J. E. 2001. Synthesis, structure, mechanical properties, and thermal stability of some polysulfone/organoclay nanocomposite. Polymer, 42, 9783-9789.

41. Li, X., and Ha, C. 2003. Nanostructure of EVA/organoclay nanocomosites: Effects of kinds of organoclays and grafting of maleic anhydride onto EVA. Journal of Applied Polymer Science, 87, 1901-1909.

42. Zheng, J. P., Li, P.,Ma, Y. L., and Yao, K. D. 2002. Gelatin/Montmorillonite Hybrid Nanocomposite I. Preparation and Properties. Journal of Applied Polymer Science, 86, 1189-1194.

43. Arroyo, M., López-Manchado, M. A., and Herrero, B. 2003. Organo-montmorillonite as substitute of carbon black in natural rubber compounds. Polymer, 44, 2447-2453.

44. Park, H. M., Li, X., Jin, C. Z., Park, C. Y., Cho, W. J., and Ha, C. S. 2003. Environmentally friendly polymer hybrids Part I Mechanical, thermal, and

barrier properties of thermoplastic starch/clay nanocomposites. Chemistry of Materials, 38 (5), 909-915.

45. ASTM standard D882, Standard test method for tensile properties of thin plastic sheeting. Annual Book of ASTM Standards, ASTM 08.01.

46. ISO standard 2528-1995E, Sheet materials – Determination of water vapour transmission rate – Gravimetric (dish) method. International Organization for Standardization, ISO.

47. Morgan, A. B., Gilman, J. W. 2003. Characterization of polymer-layered silicate (clay) nanocomposites by transmission electron microscopy and X-ray diffraction study, Journal of Applied Polymer Science, 87, 1329-1338.

48. Usuki, A., Kawasumi, M., Kojima, Y., Okada, A., Kurauchi, T., and Kamigaito, O. 1992. Swelling behavior of montmorillonite cation exchanged for ω-amino acids by ε–caprolactam, Journal of Materials Research, 8(5), 1174-1180.

APPENDICES

APPENDIX A

Table A Effect of diethanolamine content on the viscosity (cps) of montmorillonite dispersion at rotational speed 20 rpm

MMT:DEA	Spindle No.	Analyze No.	Reading value	Factor	Viscosity (cps)	Average (cps)	SD (cps)
10:0.0	2	1	13.25	20	265	266	4.18
		2	13.25	20	265		
		3	13.50	20	270		
		4	13.50	20	270		
		5	13.00	20	260		
10:0.5	3	1	28.00	50	1400	1410	13.69
		2	28.50	50	1425		
		3	28.50	50	1425		
		4	28.00	50	1400		
		5	28.00	50	1400		
10:1.0	5	1	11.50	200	2300	2280	44.72
		2	11.00	200	2200		
		3	11.50	200	2300		
		4	11.50	200	2300		
		5	11.50	200	2300		
10:2.0	5	1	23.50	200	4700	4710	54.77
		2	23.50	200	4700		
		3	23.50	200	4700		
		4	24.00	200	4800		
		5	23.25	200	4650		
10:3.0	5	1	28.50	200	5700	5740	54.77
		2	29.00	200	5800		
		3	28.50	200	5700		
		4	28.50	200	5700		
		5	29.00	200	5800		
10:4.0	5	1	30.50	200	6100	6040	41.83
		2	30.25	200	6050		
		3	30.25	200	6050		
		4	30.00	200	6000		
		5	30.00	200	6000		
10:5.0	5	1	32.00	200	6400	6540	114.02
		2	33.50	200	6700		
		3	32.50	200	6500		
		4	32.50	200	6500		
		5	33.00	200	6600		

Table A (continued) Effect of diethanolamine content on the viscosity (cps) of montmorillonite dispersion at rotational speed 20 rpm

MMT:DEA	Spindle No.	Analyze No.	Reading value	Factor	Viscosity (cps)	Average (cps)	SD (cps)
10:6.0	5	1 2 3 4 5	32.50 33.00 33.00 33.50 33.00	200 200 200 200 200	6500 6600 6600 6700 6600	6600	70.71
10:7.0	5	1 2 3 4 5	32.50 32.00 32.50 32.50 33.50	200 200 200 200 200	6500 6400 6500 6500 6700	6520	109.54
10:8.0	5	1 2 3 4 5	32.50 33.00 33.50 33.00 33.50	200 200 200 200 200	6500 6600 6700 6600 6700	6620	83.67

APPENDIX B

Table B Thickness of cassava starch/montmorillonite nanocomposite films

Formula	Thickness (μm)					Formula	Thickness (μm)				
	No.1	**No.2**	**No.3**	**No.4**	**No.5**		**No.1**	**No.2**	**No.3**	**No.4**	**No.5**
St-C0,D0	71.6	70.2	61.8	66.8	73.9	St-C2,D1	70.5	73.5	73.7	67.3	71.0
	72.5	73.4	72.2	69.4	74.5		71.4	67.9	71.6	71.5	71.8
	70.9	77.2	73.4	76.3	73.3		68.7	67.0	67.3	68.9	70.5
	76.7	74.7	64.6	70.2	68.9		72.4	64.4	74.6	70.3	73.7
	62.4	63.9	70.2	70.8	70.5		68.7	69.4	80.2	71.5	72.2
	71.0	76.3	63.2	71.4	70.7		69.4	74.0	71.9	70.7	70.4
	67.8	68.2	71.8	69.7	70.6		67.7	73.3	69.9	73.8	68.8
	69.6	62.5	73.5	75.3	71.4		72.6	68.9	70.0	68.6	68.0
	70.0	71.0	73.7	74.7	71.2		76.4	74.9	73.4	69.8	66.7
	73.1	72.8	62.7	68.7	68.5		68.9	69.2	74.0	75.7	73.4
	73.3	70.5	71.6	80.9	70.0		68.9	67.9	72.2	77.4	70.9
	77.1	70.1	71.8	74.5	76.5		69.6	68.3	75.8	76.5	73.4
	74.3	74.7	73.5	68.0	77.2		68.0	73.0	75.6	70.0	67.7
	72.0	80.2	73.7	65.9	69.9		79.0	72.0	68.2	70.4	72.5
	71.7	72.6	62.7	70.7	65.3		76.7	75.4	67.3	70.5	73.8
Mean	71.6	71.9	69.4	71.6	71.5	Mean	71.3	70.6	72.4	71.5	71.0
Average Mean	71.2					Average Mean	71.4				
SD	4.09					SD	3.14				

Table B (continued) Thickness of cassava starch/montmorillonite nanocomposite films

Formula	Thickness (μm)					Formula	Thickness (μm)				
	No.1	**No.2**	**No.3**	**No.4**	**No.5**		**No.1**	**No.2**	**No.3**	**No.4**	**No.5**
St-C4,D2	71.6	70.2	72.4	68.9	76.8	St-C6,D3	72.0	69.2	70.4	66.9	75.8
	72.5	69.5	71.1	70.7	74.5		70.2	70.5	69.1	71.7	71.5
	75.2	67.0	72.1	73.0	69.9		72.2	70.7	71.1	72.5	72.9
	75.1	75.5	71.4	71.0	73.2		74.8	73.6	72.4	71.5	74.1
	70.9	76.5	69.7	70.1	68.8		71.7	75.5	66.7	70.6	71.5
	76.0	75.4	74.9	71.4	70.3		66.7	75.4	74.9	71.7	70.3
	70.0	69.3	72.3	69.4	70.7		70.8	69.3	77.4	70.4	75.0
	67.9	71.4	71.7	69.1	69.9		72.8	71.7	71.7	66.6	70.9
	68.0	69.0	73.5	70.5	67.5		64.2	63.8	73.5	70.6	69.5
	70.4	71.3	73.9	73.0	71.2		69.9	72.3	71.4	76.0	71.3
	69.8	74.8	68.7	74.0	75.1		67.9	71.7	70.0	75.0	72.0
	75.3	70.3	71.2	74.1	73.3		73.8	71.3	71.5	73.1	74.5
	65.6	70.7	68.3	67.8	72.0		76.2	65.7	67.3	67.6	75.0
	69.3	70.3	67.7	75.4	67.3		74.8	70.3	75.7	73.4	64.6
	67.7	70.0	69.7	77.2	70.0		67.6	71.0	68.5	73.2	72.0
Mean	71.0	71.4	71.2	71.7	71.4	Mean	71.0	70.8	71.4	71.4	72.1
Average Mean	71.3					Average Mean	71.3				
SD	2.67					SD	2.96				

Table B (continued) Thickness of cassava starch/montmorillonite nanocomposite films

Formula	Thickness (μm)					Formula	Thickness (μm)				
	No.1	**No.2**	**No.3**	**No.4**	**No.5**		**No.1**	**No.2**	**No.3**	**No.4**	**No.5**
St-C8,D4	75.6	70.2	75.7	64.3	73.0	St-C10,D5	62.7	64.8	66.9	73.5	71.9
	74.3	77.9	70.5	71.5	70.8		68.3	72.2	69.9	75.5	73.5
	70.5	71.2	66.3	68.9	71.4		67.7	73.4	76.3	70.4	71.3
	67.8	69.5	75.6	73.3	75.7		71.2	64.6	71.2	68.9	67.9
	62.8	68.9	80.3	71.5	72.8		70.8	72.2	74.8	70.5	69.5
	73.1	71.4	70.9	70.7	76.4		72.8	67.0	70.4	71.7	67.7
	72.0	65.4	68.8	77.8	68.5		72.2	72.8	73.7	72.5	72.6
	75.6	67.7	70.1	68.6	68.6		80.5	73.5	75.9	73.3	74.4
	77.7	77.9	72.5	69.0	66.0		72.9	73.1	75.1	71.2	70.2
	72.9	72.1	75.0	75.3	73.4		75.1	67.7	69.7	67.5	67.5
	73.0	73.4	64.2	77.1	70.7		70.4	70.6	80.9	74.0	69.0
	73.6	67.5	67.8	76.8	73.8		73.3	71.4	74.5	75.5	76.5
	72.5	75.9	70.4	70.3	64.4		71.0	73.6	68.0	77.2	74.2
	66.4	70.2	71.2	87.4	70.5		68.0	74.5	72.3	71.4	65.9
	67.0	70.0	68.3	72.5	74.8		67.8	70.3	70.0	69.9	66.3
Mean	71.7	71.3	71.2	73.0	71.4	Mean	71.0	70.8	72.6	72.2	70.6
Average Mean	71.7					Average Mean	71.4				
SD	4.14					SD	3.42				

Table B (continued) Thickness of cassava starch/montmorillonite nanocomposite films

Formula	Thickness (μm)				
	No.1	**No.2**	**No.3**	**No.4**	**No.5**
St-C12,D6	63.4	66.8	65.9	77.5	72.9
	69.2	72.1	68.8	72.6	73.7
	66.6	73.4	80.3	71.3	70.3
	73.2	65.0	74.1	69.9	68.0
	71.7	73.2	70.8	71.6	70.5
	72.8	67.0	70.6	70.7	67.7
	75.4	72.5	70.7	72.5	70.6
	80.3	77.7	75.9	72.4	76.4
	72.0	73.3	75.7	71.2	74.5
	76.5	66.7	65.0	68.6	66.5
	69.4	71.6	80.4	70.8	68.0
	73.5	71.1	74.5	75.5	77.5
	72.2	74.0	67.4	74.2	73.5
	69.0	73.5	72.3	75.4	65.8
	66.8	70.3	71.2	69.9	66.6
Mean	71.5	71.2	72.2	72.3	70.8
Average Mean	71.6				
SD	3.73				

APPENDIX C

Table C Average of tensile properties of various films at various MMT, DEA contents

Formula	No.	Thickness (mm)	Tensile strength (MPa)	%Elongation at break (%)	Young's Modulus (MPa)
St-C0,D0	1	0.075	18.34	4.84	751.64
	2	0.074	18.14	5.45	740.41
	3	0.063	19.07	4.38	750.79
	4	0.080	18.36	4.18	740.32
	5	0.079	18.69	3.82	759.76
Mean		**0.074**	**18.52**	**4.53**	**748.58**
SD		**0.007**	**0.37**	**0.63**	**8.28**
St-C2,D1	1	0.065	12.48	7.47	533.33
	2	0.069	12.68	6.84	556.14
	3	0.073	12.15	6.41	523.71
	4	0.073	12.77	6.83	538.82
	5	0.071	12.66	7.95	534.18
Mean		**0.070**	**12.55**	**7.10**	**537.24**
SD		**0.003**	**0.25**	**0.61**	**11.91**
St-C4,D2	1	0.074	11.41	10.34	438.85
	2	0.068	12.66	10.10	458.17
	3	0.076	10.13	13.27	440.70
	4	0.073	11.89	9.32	430.80
	5	0.076	11.28	9.52	437.21
Mean		**0.073**	**11.47**	**10.51**	**441.15**
SD		**0.003**	**0.93**	**1.60**	**10.22**
St-C6,D3	1	0.075	9.88	17.84	387.22
	2	0.074	9.06	19.53	396.40
	3	0.072	7.76	18.20	383.67
	4	0.071	9.21	18.45	404.52
	5	0.081	9.79	18.43	389.40
Mean		**0.075**	**9.14**	**18.49**	**392.24**
SD		**0.004**	**0.85**	**0.63**	**8.29**
St-C8,D4	1	0.065	5.28	27.17	202.97
	2	0.077	5.56	28.60	211.94
	3	0.070	5.96	26.81	214.53
	4	0.075	5.08	27.23	197.51
	5	0.079	5.61	27.42	199.61
Mean		**0.073**	**5.50**	**27.45**	**205.31**
SD		**0.006**	**0.34**	**0.68**	**7.55**

Table C (continued) Average of tensile properties of various films at various MMT, DEA contents

Formula	No.	Thickness (mm)	Tensile strength (MPa)	%Elongation at break (%)	Young's Modulus (MPa)
St-C10,D5	1	0.063	4.71	32.56	146.56
	2	0.072	5.34	33.80	146.38
	3	0.069	5.08	35.22	155.24
	4	0.070	5.08	32.08	155.72
	5	0.067	5.04	37.70	154.98
Mean		**0.068**	**5.05**	**34.27**	**151.78**
SD		**0.003**	**0.22**	**2.27**	**4.85**
St-C12,D6	1	0.067	4.48	44.02	101.77
	2	0.074	5.43	41.09	112.38
	3	0.080	4.53	43.93	103.12
	4	0.063	5.09	43.91	115.92
	5	0.076	4.46	42.73	104.41
Mean		**0.072**	**4.80**	**43.14**	**107.52**
SD		**0.007**	**0.44**	**1.26**	**6.25**
St-C0,D1	1	0.065	11.19	8.92	467.15
	2	0.070	10.71	9.29	470.98
	3	0.071	10.42	10.17	456.76
	4	0.068	10.94	9.04	466.57
	5	0.065	10.05	10.02	460.33
Mean		**0.068**	**10.66**	**9.49**	**464.36**
SD		**0.003**	**0.45**	**0.57**	**5.71**
St-C0,D2	1	0.072	9.67	15.03	393.15
	2	0.070	10.58	12.23	397.56
	3	0.071	10.39	12.39	413.67
	4	0.068	9.71	13.71	408.35
	5	0.071	9.94	12.43	416.80
Mean		**0.070**	**10.06**	**13.16**	**405.91**
SD		**0.002**	**0.41**	**1.20**	**10.21**
St-C0,D3	1	0.066	8.07	22.76	250.13
	2	0.063	8.35	21.84	258.56
	3	0.071	7.88	24.76	244.75
	4	0.067	8.18	23.84	257.84
	5	0.071	7.83	22.31	249.33
Mean		**0.068**	**8.06**	**23.10**	**252.12**
SD		**0.003**	**0.21**	**1.19**	**5.92**

Table C (continued) Average of tensile properties of various films at various MMT, DEA contents

Formula	No.	Thickness (mm)	Tensile strength (MPa)	%Elomgation at break (%)	Young's Modulus (MPa)
St-C0,D4	1	0.073	5.92	30.76	161.31
	2	0.070	5.30	30.44	168.57
	3	0.072	5.95	31.53	158.48
	4	0.071	5.64	32.40	153.39
	5	0.068	5.47	34.42	147.43
Mean		**0.071**	**5.66**	**31.91**	**157.84**
SD		**0.002**	**0.28**	**1.59**	**8.00**
St-C0,D5	1	0.065	5.21	40.48	137.43
	2	0.064	5.33	39.85	143.57
	3	0.068	4.98	42.53	147.45
	4	0.067	5.37	39.33	132.97
	5	0.066	5.01	40.93	132.88
Mean		**0.066**	**5.18**	**40.62**	**138.86**
SD		**0.002**	**0.18**	**1.23**	**6.49**
St-C0,D6	1	0.068	4.17	47.83	89.34
	2	0.070	4.38	46.75	86.67
	3	0.071	4.13	44.51	82.89
	4	0.069	4.01	46.34	86.77
	5	0.073	4.22	46.92	84.84
Mean		**0.070**	**4.18**	**46.47**	**86.10**
SD		**0.002**	**0.14**	**1.22**	**2.41**
St-C2,D0	1	0.068	19.18	4.06	773.46
	2	0.066	18.61	4.27	753.45
	3	0.066	18.54	3.78	756.73
	4	0.067	18.20	3.86	745.97
	5	0.067	18.67	4.62	745.92
Mean		**0.067**	**18.64**	**4.12**	755.11
SD		0.001	0.35	0.34	11.29
St-C4,D0	1	0.068	18.95	3.91	756.74
	2	0.069	19.00	3.93	760.12
	3	0.069	18.96	3.63	753.34
	4	0.072	19.64	4.27	769.48
	5	0.071	19.12	3.67	765.72
Mean		0.070	19.13	3.88	761.08
SD		0.002	0.29	0.26	6.55

Table C (continued) Average of tensile properties of various films at various MMT, DEA contents

Formula	No.	Thickness (mm)	Tensile strength (MPa)	%Elongation at break (%)	Young's Modulus (MPa)
St-C6,D0	1	0.071	19.68	4.09	754.85
	2	0.070	18.71	4.17	764.12
	3	0.071	20.05	3.86	762.40
	4	0.069	19.46	3.83	764.87
	5	0.072	19.46	3.34	767.34
Mean		**0.071**	**19.51**	**3.86**	**762.72**
SD		**0.001**	**0.50**	**0.32**	**4.74**
St-C8,D0	1	0.072	18.16	3.84	747.01
	2	0.071	19.38	3.82	757.23
	3	0.069	19.85	4.16	764.42
	4	0.073	18.71	3.38	757.48
	5	0.073	19.13	3.48	760.04
Mean		**0.072**	**19.05**	**3.74**	**757.24**
SD		**0.002**	**0.65**	**0.31**	**6.41**
St-C10,D0	1	0.072	17.91	3.35	742.55
	2	0.071	19.64	3.62	762.24
	3	0.070	18.76	3.22	756.27
	4	0.069	20.06	3.11	771.45
	5	0.068	18.45	3.47	755.23
Mean		**0.070**	**18.96**	**3.35**	**757.55**
SD		**0.002**	**0.88**	**0.20**	**10.57**
St-C12,D0	1	0.066	17.78	3.10	748.05
	2	0.066	18.50	3.21	759.83
	3	0.067	18.06	3.52	755.48
	4	0.069	18.86	3.18	760.55
	5	0.070	18.89	3.32	753.32
Mean		**0.068**	**18.42**	**3.27**	**755.45**
SD		**0.002**	**0.49**	**0.16**	**5.11**

APPENDIX D

Table D Transparency of starch film and nanocomposite film

Formula Standard

Wavelength (nm)	Transmittance (%)			
	No.1	No.2	No.3	Mean
360	73.312	73.259	73.106	73.226
370	80.472	80.509	80.585	80.522
380	85.693	85.888	85.693	85.758
390	89.852	89.921	89.761	89.845
400	93.008	93.028	92.93	92.989
410	94.869	94.971	94.898	94.913
420	95.875	95.983	95.873	95.910
430	96.458	96.455	96.470	96.461
440	96.552	96.576	96.491	96.540
450	96.788	96.839	96.617	96.748
460	97.055	97.158	96.980	97.064
470	97.336	97.348	97.228	97.304
480	97.338	97.418	97.358	97.371
490	97.498	97.487	97.420	97.468
500	97.548	97.545	97.505	97.533
510	97.456	97.54	97.470	97.489
520	97.451	97.486	97.414	97.450
530	97.418	97.421	97.400	97.413
540	97.373	97.405	97.399	97.392
550	97.293	97.350	97.273	97.305
560	97.131	97.198	97.151	97.160
570	96.945	96.997	96.983	96.975
580	96.765	96.872	96.756	96.798
590	96.728	96.744	96.717	96.730
600	96.760	96.827	96.799	96.795
610	96.714	96.815	96.746	96.758
620	96.674	96.659	96.675	96.669
630	96.546	96.686	96.614	96.615
640	96.535	96.581	96.543	96.553
650	96.451	96.502	96.443	96.465
660	96.489	96.538	96.416	96.481
670	96.574	96.624	96.543	96.580
680	96.540	96.638	96.600	96.593
690	96.467	96.567	96.454	96.496
700	96.467	96.537	96.479	96.494
710	96.444	96.519	96.461	96.475
720	96.333	96.495	96.390	96.406
730	96.291	96.469	96.300	96.353
740	96.174	96.273	96.226	96.224
750	96.105	96.186	96.105	96.132

Table D (continued) Transparency of starch film and nanocomposite film.

Formula St-C0,D0

Wavelength (nm)	Transmittance (%)			
	No.1	No.2	No.3	Mean
360	70.443	70.548	70.450	70.480
370	77.064	77.245	77.148	77.152
380	82.249	82.282	82.208	82.246
390	86.449	86.472	86.424	86.448
400	89.721	89.752	89.667	89.713
410	91.788	91.822	91.742	91.784
420	92.999	93.020	92.943	92.987
430	93.683	93.694	93.618	93.665
440	93.910	93.878	93.829	93.872
450	94.264	94.285	94.181	94.243
460	94.618	94.636	94.538	94.597
470	94.957	94.965	94.893	94.938
480	95.094	95.041	94.982	95.039
490	95.287	95.260	95.186	95.244
500	95.385	95.375	95.309	95.356
510	95.356	95.365	95.289	95.337
520	95.419	95.375	95.306	95.367
530	95.499	95.440	95.378	95.439
540	95.462	95.423	95.352	95.412
550	95.504	95.418	95.357	95.426
560	95.373	95.283	95.219	95.292
570	95.291	95.191	95.106	95.196
580	95.095	94.999	94.935	95.010
590	95.076	94.981	94.943	95.000
600	95.172	95.088	95.009	95.090
610	95.147	95.039	94.984	95.057
620	95.126	95.029	94.950	95.035
630	95.010	94.925	94.881	94.939
640	95.046	94.933	94.869	94.939
650	94.979	94.859	94.804	94.881
660	95.055	94.947	94.861	94.954
670	95.138	95.000	94.961	95.033
680	95.104	95.005	94.959	95.023
690	95.069	94.954	94.899	94.974
700	95.093	94.983	94.929	95.002
710	95.073	94.952	94.919	94.981
720	94.988	94.874	94.846	94.903
730	94.948	94.832	94.810	94.863
740	94.822	94.726	94.690	94.746
750	94.751	94.644	94.611	94.669

Table D (continued) Transparency of starch film and nanocomposite film

Formula St-C2,D1

Wavelength (nm)	Transmittance (%)			
	No.1	No.2	No.3	Mean
360	64.288	64.084	64.122	64.165
370	70.905	70.505	70.629	70.680
380	75.789	75.518	75.591	75.633
390	79.946	79.809	79.935	79.897
400	83.395	83.235	83.302	83.311
410	85.815	85.643	85.705	85.721
420	87.351	87.237	87.271	87.286
430	88.463	88.394	88.405	88.421
440	89.012	89.004	89.073	89.030
450	89.680	89.765	89.778	89.741
460	90.483	90.529	90.504	90.505
470	91.029	91.025	91.026	91.027
480	91.490	91.377	91.370	91.412
490	91.742	91.792	91.775	91.770
500	92.077	92.087	92.081	92.082
510	92.254	92.144	92.156	92.185
520	92.377	92.312	92.328	92.339
530	92.560	92.561	92.544	92.555
540	92.804	92.689	92.670	92.721
550	92.896	92.898	92.864	92.886
560	92.989	92.948	92.889	92.942
570	93.079	93.053	92.990	93.041
580	93.064	93.028	92.963	93.018
590	93.219	93.155	93.075	93.150
600	93.475	93.417	93.334	93.409
610	93.587	93.496	93.360	93.481
620	93.592	93.575	93.436	93.534
630	93.672	93.582	93.416	93.557
640	93.728	93.674	93.482	93.628
650	93.690	93.669	93.506	93.622
660	93.776	93.779	93.586	93.714
670	93.946	93.939	93.791	93.892
680	94.112	94.012	93.853	93.992
690	94.039	93.990	93.807	93.945
700	94.109	94.041	93.878	94.009
710	94.135	94.067	93.906	94.036
720	94.106	94.011	93.827	93.981
730	94.096	94.016	93.828	93.980
740	94.016	93.931	93.752	93.900
750	93.927	93.920	93.733	93.860

Table D (continued) Transparency of starch film and nanocomposite film

Formula St-C4,D2

Wavelength (nm)	Transmittance (%)			
	No.1	No.2	No.3	Mean
360	63.155	63.114	63.674	63.314
370	69.776	69.537	70.096	69.803
380	74.798	74.496	75.244	74.846
390	79.015	78.796	79.498	79.103
400	82.473	82.205	82.936	82.538
410	84.878	84.578	85.322	84.926
420	86.395	86.123	86.851	86.456
430	87.532	87.247	87.949	87.576
440	88.176	87.958	88.534	88.223
450	88.826	88.677	89.257	88.920
460	89.672	89.406	89.927	89.668
470	90.237	89.948	90.437	90.207
480	90.662	90.308	90.726	90.565
490	90.996	90.751	91.130	90.959
500	91.325	91.020	91.417	91.254
510	91.516	91.175	91.519	91.403
520	91.673	91.368	91.671	91.571
530	91.890	91.625	91.904	91.806
540	92.167	91.756	92.081	92.001
550	92.301	92.011	92.291	92.201
560	92.433	92.113	92.368	92.305
570	92.537	92.248	92.475	92.420
580	92.579	92.243	92.508	92.443
590	92.741	92.402	92.657	92.600
600	93.011	92.722	92.940	92.891
610	93.140	92.832	93.058	93.010
620	93.158	92.915	93.116	93.063
630	93.290	92.937	93.170	93.132
640	93.339	93.016	93.234	93.196
650	93.309	93.050	93.275	93.211
660	93.377	93.170	93.364	93.304
670	93.627	93.396	93.584	93.536
680	93.731	93.462	93.661	93.618
690	93.703	93.440	93.638	93.594
700	93.801	93.525	93.704	93.677
710	93.847	93.563	93.778	93.729
720	93.816	93.526	93.698	93.680
730	93.800	93.508	93.701	93.670
740	93.736	93.420	93.593	93.583
750	93.650	93.426	93.603	93.560

Table D (continued) Transparency of starch film and nanocomposite film

Formula St-C6,D3

Wavelength (nm)	Transmittance (%)			
	No.1	No.2	No.3	Mean
360	60.743	61.516	61.794	61.351
370	67.055	67.816	68.162	67.678
380	72.112	72.894	73.239	72.748
390	76.354	77.090	77.416	76.953
400	79.802	80.487	80.901	80.397
410	82.291	82.893	83.257	82.814
420	83.913	84.447	84.838	84.399
430	85.086	85.598	85.990	85.558
440	85.891	86.323	86.715	86.310
450	86.669	87.013	87.410	87.031
460	87.410	87.827	88.262	87.833
470	88.158	88.434	88.877	88.490
480	88.637	88.866	89.303	88.935
490	89.073	89.277	89.714	89.355
500	89.417	89.582	90.023	89.674
510	89.699	89.860	90.261	89.940
520	89.934	90.066	90.481	90.160
530	90.257	90.391	90.795	90.481
540	90.581	90.664	91.099	90.781
550	90.867	90.914	91.357	91.046
560	91.095	91.082	91.529	91.235
570	91.220	91.207	91.632	91.353
580	91.439	91.368	91.813	91.540
590	91.694	91.559	91.980	91.744
600	92.012	91.837	92.289	92.046
610	92.263	92.063	92.517	92.281
620	92.317	92.123	92.597	92.346
630	92.462	92.188	92.673	92.441
640	92.608	92.325	92.780	92.571
650	92.620	92.350	92.791	92.587
660	92.764	92.444	92.892	92.700
670	92.984	92.681	93.140	92.935
680	93.150	92.867	93.295	93.104
690	93.214	92.900	93.340	93.151
700	93.330	92.964	93.430	93.241
710	93.407	93.061	93.500	93.323
720	93.382	93.034	93.477	93.298
730	93.409	93.029	93.462	93.300
740	93.347	92.971	93.421	93.246
750	93.253	92.911	93.341	93.168

Table D (continued) Transparency of starch film and nanocomposite film

Formula St-C8,D4

Wavelength (nm)	Transmittance (%)			
	No.1	No.2	No.3	Mean
360	55.459	57.195	55.459	56.038
370	62.362	64.032	62.362	62.919
380	68.361	69.938	68.361	68.887
390	73.349	74.666	73.349	73.788
400	77.202	78.455	77.202	77.620
410	79.917	81.118	79.917	80.317
420	81.754	82.849	81.754	82.119
430	83.171	84.145	83.171	83.496
440	84.126	85.052	84.126	84.435
450	85.047	85.888	85.047	85.327
460	86.099	86.873	86.099	86.357
470	86.881	87.549	86.881	87.104
480	87.375	88.068	87.375	87.606
490	87.938	88.587	87.938	88.154
500	88.409	88.99	88.409	88.603
510	88.754	89.282	88.754	88.930
520	89.062	89.568	89.062	89.231
530	89.461	89.964	89.461	89.629
540	89.839	90.268	89.839	89.982
550	90.231	90.621	90.231	90.361
560	90.498	90.858	90.498	90.618
570	90.687	91.004	90.687	90.793
580	90.995	91.251	90.995	91.080
590	91.255	91.464	91.255	91.325
600	91.624	91.812	91.624	91.687
610	91.917	92.083	91.917	91.972
620	92.062	92.181	92.062	92.102
630	92.147	92.255	92.147	92.183
640	92.279	92.394	92.279	92.317
650	92.337	92.390	92.337	92.355
660	92.428	92.498	92.428	92.451
670	92.723	92.767	92.723	92.738
680	92.926	92.959	92.926	92.937
690	92.945	93.019	92.945	92.970
700	93.040	93.114	93.040	93.065
710	93.153	93.231	93.153	93.179
720	93.142	93.201	93.142	93.162
730	93.164	93.243	93.164	93.190
740	93.133	93.207	93.133	93.158
750	93.052	93.127	93.052	93.077

Table D (continued) Transparency of starch film and nanocomposite film

Formula St-C10,D5

Wavelength (nm)	Transmittance (%)			
	No.1	No.2	No.3	Mean
360	57.992	57.364	58.012	57.789
370	64.151	63.503	64.172	63.942
380	69.256	68.526	69.224	69.002
390	73.598	72.904	73.617	73.373
400	77.167	76.481	77.192	76.947
410	79.759	79.020	79.731	79.503
420	81.509	80.788	81.460	81.252
430	82.767	82.089	82.691	82.516
440	83.639	82.979	83.581	83.400
450	84.473	83.829	84.425	84.242
460	85.419	84.794	85.412	85.208
470	86.141	85.538	86.096	85.925
480	86.664	86.040	86.595	86.433
490	87.096	86.535	87.074	86.902
500	87.487	86.971	87.486	87.315
510	87.837	87.273	87.804	87.638
520	88.175	87.645	88.145	87.988
530	88.574	88.069	88.517	88.387
540	88.946	88.485	88.966	88.799
550	89.326	88.894	89.333	89.184
560	89.685	89.245	89.651	89.527
570	89.949	89.531	89.912	89.797
580	90.273	89.865	90.247	90.128
590	90.621	90.245	90.590	90.485
600	91.018	90.672	90.975	90.888
610	91.305	90.976	91.319	91.200
620	91.481	91.134	91.469	91.361
630	91.644	91.316	91.599	91.520
640	91.838	91.502	91.811	91.717
650	91.894	91.607	91.904	91.802
660	92.025	91.781	92.031	91.946
670	92.315	92.048	92.327	92.230
680	92.560	92.287	92.565	92.471
690	92.640	92.401	92.641	92.561
700	92.782	92.541	92.782	92.702
710	92.875	92.648	92.920	92.814
720	92.899	92.695	92.898	92.831
730	92.916	92.709	92.970	92.865
740	92.923	92.703	92.942	92.856
750	92.866	92.635	92.877	92.793

Table D (continued) Transparency of starch film and nanocomposite film

Formula St-C12,D6

Wavelength (nm)	Transmittance (%)			
	No.1	No.2	No.3	Mean
360	55.300	55.590	53.245	54.712
370	61.412	61.717	59.463	60.864
380	66.447	66.697	64.393	65.846
390	70.769	70.984	68.634	70.129
400	74.281	74.556	72.236	73.691
410	76.821	77.106	74.877	76.268
420	78.689	78.931	76.781	78.134
430	80.033	80.246	78.285	79.521
440	80.995	81.168	79.326	80.496
450	81.970	82.150	80.385	81.502
460	82.984	83.133	81.568	82.562
470	83.756	83.931	82.420	83.369
480	84.316	84.451	83.082	83.950
490	84.886	85.006	83.689	84.527
500	85.384	85.492	84.289	85.055
510	85.748	85.845	84.727	85.440
520	86.156	86.235	85.178	85.856
530	86.632	86.705	85.665	86.334
540	87.058	87.116	86.219	86.798
550	87.573	87.621	86.737	87.310
560	88.018	88.088	87.234	87.780
570	88.481	88.571	87.774	88.275
580	88.891	88.949	88.226	88.689
590	89.326	89.438	88.720	89.161
600	89.898	89.951	89.314	89.721
610	90.200	90.237	89.659	90.032
620	90.523	90.560	89.876	90.320
630	90.622	90.681	90.108	90.470
640	90.827	90.894	90.306	90.676
650	90.962	91.035	90.407	90.801
660	91.212	91.300	90.644	91.052
670	91.519	91.585	90.974	91.359
680	91.671	91.761	91.246	91.559
690	91.800	91.898	91.306	91.668
700	91.918	92.026	91.489	91.811
710	92.042	92.158	91.606	91.935
720	92.087	92.168	91.701	91.985
730	92.155	92.257	91.755	92.056
740	92.103	92.244	91.757	92.035
750	92.127	92.252	91.736	92.038

Table D (continued) Transparency of starch film and nanocomposite film

Formula St-C2,D0

Wavelength (nm)	Transmittance (%)			
	No.1	No.2	No.3	Mean
360	63.446	62.143	62.124	62.571
370	70.032	68.718	68.748	69.166
380	75.343	74.063	74.029	74.478
390	79.578	78.296	78.267	78.714
400	83.098	81.797	81.783	82.226
410	85.544	84.357	84.282	84.728
420	87.193	86.119	86.040	86.451
430	88.370	87.342	87.208	87.640
440	89.076	88.160	88.013	88.416
450	89.851	88.992	88.849	89.231
460	90.594	89.814	89.665	90.024
470	91.227	90.458	90.299	90.661
480	91.639	90.899	90.694	91.077
490	91.951	91.302	91.093	91.449
500	92.265	91.601	91.394	91.753
510	92.486	91.871	91.651	92.003
520	92.676	92.088	91.845	92.203
530	92.855	92.305	92.036	92.399
540	93.086	92.588	92.340	92.671
550	93.259	92.814	92.559	92.877
560	93.378	92.966	92.678	93.007
570	93.444	93.038	92.723	93.068
580	93.547	93.147	92.887	93.194
590	93.564	93.250	92.923	93.246
600	93.874	93.536	93.242	93.551
610	94.023	93.696	93.392	93.704
620	93.972	93.722	93.411	93.702
630	94.149	93.930	93.535	93.871
640	94.112	93.891	93.562	93.855
650	94.137	93.930	93.582	93.883
660	94.262	94.049	93.686	93.999
670	94.431	94.238	93.881	94.183
680	94.464	94.320	93.963	94.249
690	94.493	94.315	93.961	94.256
700	94.517	94.359	93.994	94.290
710	94.497	94.369	94.043	94.303
720	94.535	94.395	94.071	94.334
730	94.535	94.426	94.101	94.354
740	94.405	94.255	93.955	94.205
750	94.307	94.196	93.868	94.124

Table D (continued) Transparency of starch film and nanocomposite film

Formula St-C4,D0

Wavelength (nm)	Transmittance (%)			
	No.1	No.2	No.3	Mean
360	61.291	60.407	61.227	60.975
370	67.791	66.808	67.756	67.452
380	73.029	72.136	73.024	72.730
390	77.262	76.370	77.261	76.964
400	80.811	79.891	80.747	80.483
410	83.285	82.448	83.292	83.008
420	85.046	84.226	84.999	84.757
430	86.257	85.524	86.233	86.005
440	87.162	86.381	87.059	86.867
450	87.936	87.301	87.923	87.720
460	88.817	88.211	88.788	88.605
470	89.503	88.885	89.443	89.277
480	89.969	89.398	89.903	89.757
490	90.376	89.846	90.285	90.169
500	90.755	90.234	90.648	90.546
510	91.073	90.558	90.900	90.844
520	91.294	90.826	91.197	91.106
530	91.553	91.089	91.442	91.361
540	91.882	91.455	91.750	91.696
550	92.130	91.742	92.022	91.965
560	92.333	91.961	92.216	92.170
570	92.450	92.095	92.304	92.283
580	92.620	92.296	92.502	92.473
590	92.731	92.401	92.649	92.594
600	93.075	92.797	92.981	92.951
610	93.260	93.007	93.149	93.139
620	93.289	93.023	93.189	93.167
630	93.457	93.179	93.386	93.341
640	93.488	93.228	93.389	93.368
650	93.523	93.261	93.438	93.407
660	93.639	93.412	93.560	93.537
670	93.871	93.625	93.784	93.760
680	93.962	93.751	93.884	93.866
690	93.974	93.760	93.885	93.873
700	93.982	93.774	93.935	93.897
710	94.060	93.852	93.984	93.912
720	94.051	93.859	93.989	93.966
730	94.096	93.889	94.002	93.996
740	93.945	93.763	93.871	93.860
750	93.865	93.692	93.827	93.795

Table D (continued) Transparency of starch film and nanocomposite film

Formula St-C6,D0

Wavelength (nm)	Transmittance (%)			
	No.1	No.2	No.3	Mean
360	57.844	58.801	57.370	58.005
370	64.135	65.136	63.659	64.310
380	69.434	70.372	68.939	69.582
390	73.638	74.629	73.149	73.805
400	77.215	78.209	76.674	77.366
410	79.854	80.805	79.352	80.004
420	81.752	82.637	81.281	81.890
430	83.106	83.954	82.676	83.245
440	84.157	84.943	83.684	84.261
450	85.098	85.856	84.732	85.229
460	86.103	86.822	85.719	86.215
470	86.929	87.584	86.537	87.017
480	87.583	88.152	87.196	87.644
490	87.906	88.653	87.578	88.046
500	88.464	89.045	88.146	88.552
510	88.878	89.410	88.546	88.945
520	89.223	89.786	88.934	89.314
530	89.569	90.061	89.320	89.650
540	90.007	90.481	89.722	90.070
550	90.302	90.826	90.072	90.400
560	90.684	91.121	90.424	90.743
570	90.966	91.308	90.693	90.989
580	91.204	91.599	90.967	91.257
590	91.478	91.803	91.235	91.505
600	91.840	92.149	91.676	91.888
610	92.083	92.383	91.881	92.116
620	92.231	92.462	91.982	92.225
630	92.384	92.653	92.202	92.413
640	92.441	92.693	92.284	92.473
650	92.532	92.768	92.349	92.550
660	92.642	92.904	92.506	92.684
670	92.924	93.157	92.752	92.944
680	93.015	93.283	92.873	93.057
690	93.104	93.309	92.970	93.128
700	93.135	93.375	93.004	93.171
710	93.196	93.445	93.053	93.231
720	93.257	93.477	93.122	93.285
730	93.292	93.527	93.163	93.327
740	93.154	93.389	93.043	93.195
750	93.138	93.354	93.018	93.170

Table D (continued) Transparency of starch film and nanocomposite film

Formula St-C8,D0

Wavelength (nm)	Transmittance (%)			
	No.1	No.2	No.3	Mean
360	55.742	55.732	56.683	56.052
370	62.086	62.000	62.930	62.339
380	67.433	67.300	68.291	67.675
390	71.738	71.639	72.562	71.980
400	75.413	75.258	76.168	75.613
410	78.089	77.989	78.824	78.301
420	80.079	79.983	80.723	80.262
430	81.526	81.424	82.152	81.701
440	82.582	82.519	83.159	82.753
450	83.658	83.566	84.194	83.806
460	84.752	84.603	85.261	84.872
470	85.571	85.455	86.088	85.705
480	86.212	86.129	86.745	86.362
490	86.689	86.517	87.143	86.783
500	87.24	87.102	87.728	87.357
510	87.708	87.558	88.150	87.805
520	88.102	88.013	88.568	88.228
530	88.504	88.373	88.918	88.598
540	88.994	88.862	89.370	89.075
550	89.427	89.299	89.769	89.498
560	89.824	89.707	90.155	89.895
570	90.158	90.046	90.445	90.216
580	90.523	90.376	90.778	90.559
590	90.831	90.699	91.062	90.864
600	91.258	91.158	91.4900	91.302
610	91.530	91.412	91.745	91.562
620	91.713	91.583	91.853	91.716
630	91.926	91.829	92.063	91.939
640	92.049	91.899	92.151	92.033
650	92.153	92.029	92.256	92.146
660	92.315	92.180	92.407	92.301
670	92.622	92.483	92.712	92.606
680	92.729	92.593	92.840	92.721
690	92.826	92.696	92.916	92.813
700	92.909	92.745	93.003	92.886
710	92.981	92.841	93.077	92.966
720	93.044	92.933	93.138	93.038
730	93.120	92.972	93.196	93.096
740	92.985	92.877	93.055	92.972
750	92.975	92.853	93.036	92.955

Table D (continued) Transparency of starch film and nanocomposite film

Formula St-C10,D0

Wavelength (nm)	Transmittance (%)			
	No.1	No.2	No.3	Mean
360	54.586	52.473	54.482	53.847
370	60.877	58.564	60.683	60.041
380	66.117	63.829	65.977	65.308
390	70.410	68.152	70.304	69.622
400	74.047	71.799	73.920	73.255
410	76.783	74.614	76.642	76.013
420	78.732	76.683	78.665	78.027
430	80.198	78.264	80.124	79.529
440	81.318	79.494	81.272	80.695
450	82.432	80.698	82.391	81.840
460	83.561	81.911	83.540	83.004
470	84.474	82.916	84.453	83.948
480	85.164	83.672	85.128	84.655
490	85.702	84.224	85.644	85.190
500	86.302	84.908	86.296	85.835
510	86.774	85.431	86.743	86.316
520	87.220	85.916	87.199	86.778
530	87.635	86.433	87.629	87.232
540	88.160	87.005	88.154	87.773
550	88.631	87.538	88.637	88.269
560	89.093	88.078	89.082	88.751
570	89.454	88.537	89.476	89.156
580	89.855	89.055	89.850	89.587
590	90.200	89.429	90.229	89.953
600	90.675	89.918	90.716	90.436
610	90.968	90.284	91.006	90.753
620	91.132	90.445	91.162	90.913
630	91.370	90.723	91.398	91.164
640	91.471	90.865	91.474	91.270
650	91.606	90.978	91.606	91.397
660	91.755	91.176	91.762	91.564
670	92.081	91.486	92.070	91.879
680	92.199	91.693	92.224	92.039
690	92.293	91.805	92.319	92.139
700	92.370	91.885	92.389	92.215
710	92.482	91.993	92.491	92.322
720	92.569	92.079	92.571	92.406
730	92.647	92.188	92.628	92.488
740	92.510	92.075	92.511	92.365
750	92.503	92.071	92.511	92.362

Table D (continued) Transparency of starch film and nanocomposite film

Formula St-C12,D0

Wavelength (nm)	Transmittance (%)			
	No.1	No.2	No.3	Mean
360	48.770	48.182	50.849	49.267
370	54.561	53.907	56.719	55.062
380	59.652	59.052	61.935	60.213
390	63.934	63.279	66.206	64.473
400	67.568	66.987	69.825	68.127
410	70.410	69.811	72.628	70.950
420	72.645	72.086	74.755	73.162
430	74.364	73.806	76.392	74.854
440	75.717	75.192	77.725	76.211
450	77.126	76.624	79.031	77.594
460	78.461	78.027	80.281	78.923
470	79.577	79.140	81.323	80.013
480	80.457	80.023	82.119	80.866
490	81.129	80.725	82.682	81.512
500	81.912	81.526	83.463	82.300
510	82.511	82.160	84.052	82.908
520	83.152	82.814	84.577	83.514
530	83.764	83.447	85.143	84.118
540	84.463	84.159	85.777	84.800
550	85.164	84.890	86.437	85.497
560	85.839	85.605	87.050	86.165
570	86.487	86.266	87.598	86.784
580	87.189	87.006	88.158	87.451
590	87.659	87.487	88.665	87.937
600	88.274	88.179	89.240	88.564
610	88.722	88.566	89.598	88.962
620	88.936	88.824	89.814	89.191
630	89.291	89.169	90.118	89.526
640	89.456	89.366	90.267	89.696
650	89.648	89.541	90.416	89.868
660	89.877	89.795	90.645	90.106
670	90.267	90.147	90.999	90.471
680	90.479	90.373	91.211	90.688
690	90.637	90.564	91.329	90.843
700	90.777	90.706	91.424	90.969
710	90.927	90.875	91.576	91.126
720	91.087	90.964	91.646	91.232
730	91.181	91.114	91.778	91.358
740	91.090	91.033	91.690	91.271
750	91.123	91.068	91.691	91.294

APPENDIX E

Table E The effect of MMT, DEA content to moisture absorption

Formula	No.	Initial weight (g)	Final weight (g)	Weight difference (g)	Moisture absorption (%)
St-C0,D0	1	0.1561	0.3703	0.2142	137.22
	2	0.1649	0.3869	0.2220	134.63
	3	0.1711	0.4032	0.2321	135.65
	4	0.1768	0.4187	0.2419	136.82
	5	0.1754	0.4118	0.2364	134.78
Mean		**0.1689**	**0.3982**	**0.2293**	**135.82**
SD		**0.0085**	**0.0196**	**0.0112**	**1.17**
St-C2,D1	1	0.1693	0.3972	0.2279	134.61
	2	0.1606	0.3848	0.2242	139.60
	3	0.1557	0.3676	0.2119	136.10
	4	0.1617	0.3857	0.2240	138.53
	5	0.1684	0.3916	0.2232	132.54
Mean		**0.1631**	**0.3854**	**0.2222**	**136.28**
SD		**0.0057**	**0.0111**	**0.0061**	**2.87**
St-C4,D2	1	0.1646	0.3893	0.2237	135.91
	2	0.1501	0.3582	0.2081	138.64
	3	0.1565	0.3762	0.2197	140.38
	4	0.1593	0.3788	0.2195	137.79
	5	0.1615	0.3862	0.2247	139.13
Mean		**0.1584**	**0.3777**	**0.2191**	**138.37**
SD		**0.0055**	**0.0122**	**0.0066**	**1.66**
St-C6,D3	1	0.1683	0.3989	0.2306	137.01
	2	0.1753	0.4082	0.2329	132.86
	3	0.1649	0.3970	0.2321	140.75
	4	0.1617	0.3963	0.2346	145.08
	5	0.1730	0.4076	0.2346	135.61
Mean		**0.1686**	**0.4016**	**0.2330**	**138.26**
SD		**0.0056**	**0.0058**	**0.0017**	**4.76**
St-C8,D4	1	0.1708	0.4101	0.2393	140.10
	2	0.1666	0.4027	0.2361	141.72
	3	0.1687	0.4154	0.2467	146.24
	4	0.1722	0.4141	0.2419	140.48
	5	0.1759	0.4173	0.2414	137.24
Mean		**0.1708**	**0.4119**	**0.2411**	**141.16**
SD		**0.0035**	**0.0058**	**0.0039**	**3.28**

Table E (continued) The effect of MMT, DEA content to moisture absorption

Formula	No.	Initial weight (g)	Final weight (g)	Weight difference (g)	Moisture absorption (%)
St-C10,D5	1	0.1721	0.4151	0.2430	141.19
	2	0.1492	0.3724	0.2232	149.59
	3	0.1656	0.3958	0.2302	139.00
	4	0.1696	0.4040	0.2344	138.21
	5	0.1600	0.3815	0.2215	138.44
Mean		**0.1633**	**0.3938**	**0.2305**	**141.29**
SD		**0.0091**	**0.0171**	**0.0087**	**4.79**
St-C12,D6	1	0.1617	0.3851	0.2234	138.16
	2	0.1584	0.3861	0.2277	143.75
	3	0.1646	0.4059	0.2413	146.59
	4	0.1712	0.4101	0.2389	139.54
	5	0.1606	0.3919	0.2313	144.02
Mean		**0.1633**	**0.3958**	**0.2325**	**142.41**
SD		**0.0049**	**0.0115**	**0.0075**	**3.47**

APPENDIX F

Table F Water vapor transmission rate of cassava starch/montmorillonite nanocomposite film

No.	Formula Water vapor transmission rate ($g/m^2.day$)						
	St-C0,D0	St-C2,D1	St-C4,D2	St-C6,D3	St-C8,D4	St-C10,D5	St-C12,D6
1	2104.56	1985.52	2326.44	2114.88	2153.42	2200.80	2312.52
2	1921.44	2128.08	2108.28	2317.32	2011.78	2460.60	2440.08
3	1967.88	1927.08	1945.08	2194.80	2360.45	2030.64	2214.28
Mean	1997.96	2013.56	2126.60	2209.00	2175.22	2230.68	2322.29
SD	95.19	103.39	131.34	101.96	175.35	216.53	113.21

BIOGRAPHY

Miss Piyaporn Kampeerapappun was born on January 13, 1980 in Samutprakan, Thailand. She graduated her bachelor's degree of science in Materials Science from Faculty of Science, Chulalongkorn University in March 2001. She continued her graduated study for a master's degree of science in Applied Polymer Science and Textile Technology at the same institute in June 2001 and completed the program in April 2004.